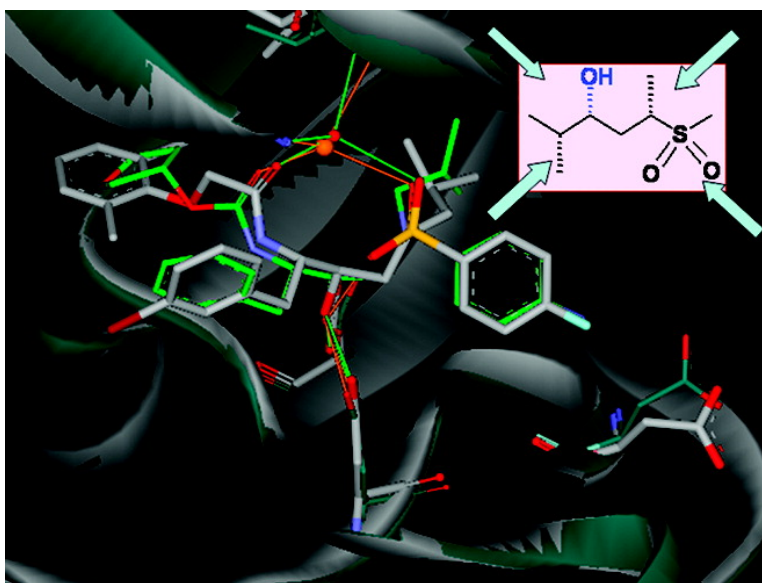


Hydroxyethylene Sulfones as a New Scaffold To Address Aspartic Proteases: Design, Synthesis, and Structural Characterization

Edgar Specker, Jark Bttcher, Andreas Heine, Christoph A. Sotriffer, Hauke Lilie, Andreas Schoop, Gerhard Mller, Nils Griebenow, and Gerhard Klebe

J. Med. Chem., **2005**, 48 (21), 6607-6619 • DOI: 10.1021/jm050224y • Publication Date (Web): 16 September 2005

Downloaded from <http://pubs.acs.org> on March 29, 2009



More About This Article

Additional resources and features associated with this article are available within the HTML version:

- Supporting Information
- Links to the 1 articles that cite this article, as of the time of this article download
- Access to high resolution figures
- Links to articles and content related to this article
- Copyright permission to reproduce figures and/or text from this article

[View the Full Text HTML](#)



Hydroxyethylene Sulfones as a New Scaffold To Address Aspartic Proteases: Design, Synthesis, and Structural Characterization

Edgar Specker, Jark Böttcher, Andreas Heine, Christoph A. Sotriffer, Hauke Lilie,[†] Andreas Schoop,[‡] Gerhard Müller,[§] Nils Griebenow,^{||} and Gerhard Klebe*

Institut für Pharmazeutische Chemie, Philipps-Universität Marburg, Marbacher Weg 6, D-35032 Marburg, Germany, Institut für Biotechnologie, Martin-Luther-Universität Halle-Wittenberg, Kurt-Mothes-Strasse 3, D-06120 Halle (Saale), Germany, Boehringer Ingelheim, Wien, Austria, Axxima Pharmaceuticals AG, München, Germany, and Bayer AG, Elberfeld, Germany

Received March 11, 2005

Hydroxyethylene sulfones were developed as novel scaffolds against aspartyl proteases. A diastereoselective synthesis has been established to introduce the required side chain decoration with desired stereochemistry. Depending on the substitution of the hydroxyethylene sulfone core, micro- to submicromolar inhibition of HIV-1 protease is achieved for the *S*-configuration at P₁ and *R*-configuration at the hydroxy-group-bearing backbone atom. This stereochemical preference is consistent with the *S,R* configuration of amprenavir. The racemic mixture of the most potent derivative (*K*_i = 80 nM) was separated by chiral HPLC, revealing the *S,R,S*-enantiomer to be more active (*K*_i = 45 nM). Docking studies suggested this isomer as the more active one. The subsequently determined crystal structure with HIV-1 protease, cocrystallized from a racemic mixture, exclusively reveals the *S,R,S*-enantiomer accommodated to the binding pocket. The transition state mimicking hydroxy group of the inhibitor is centered between both catalytic aspartates, while either its carbonyl or sulfonyl group forms H-bonds to the structurally conserved water mediating interactions between ligand and Ile50NH/Ile50NH' of both flaps. Biological testing of the stereoisomeric hydroxyethylene sulfones against cathepsin D and β -secretase did not reveal significant inhibition. Most likely, the latter proteases require inverted configuration at the hydroxy group.

Introduction

Aspartic acid proteases constitute a therapeutically relevant class of enzymes that play an important role in the regulation of various physiological processes, such as the control of blood pressure (renin),¹ digestion (pepsin),² or degradation of endocytosed proteins (cathepsin D).³ Further, they actively propagate the progression of severe diseases caused either by parasites, such as malaria (plasmepsin),⁴ or viruses, such as HIV (HIV protease),⁵ or neurodegenerative disorders including Alzheimer disease (β -secretase).⁶ On the basis of the mechanism of peptide bond hydrolysis employed by aspartate proteases, several structurally diverse transition state analogues have been designed by replacing the dipeptide-encoded scissile bond within the specific substrates. A key structural element in most transition state isosteres is a hydroxy moiety that interacts with the catalytic site aspartic acid side chains via hydrogen bonds. This secondary hydroxy group further replaces the catalytic water molecule normally bound between both aspartates and simultaneously mimics the tetrahedral geometry that is intermediately formed in the initial steps of the amide bond hydrolysis of a peptide substrate. Consequently, this type of inhibitor has been termed collected-substrate inhibitor.⁷ Figure 1 shows six well-established examples of transition state isosteres

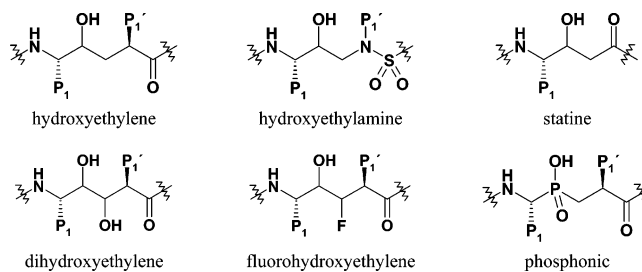


Figure 1. Examples of transition state isosteres with a hydroxy group incorporated in stable peptide bond replacements.

encompassing a noncleavable peptide bond replacement embedded in the corresponding dipeptide mimetic.

In the present contribution, we introduce a series of hydroxyethylene sulfones as novel transition state analogues. The hydroxyethylene sulfones have been synthesized and evaluated for their potential to inhibit aspartic proteases. The binding mode of one representative of the series has been crystallographically characterized together with HIV-1 protease. The novel lead structural motif has been derived from different scaffolds, already realized in known inhibitors targeting distinct aspartic proteases. The design of the novel structural motif is based on blending structural elements from known inhibitor principles into a novel structural entity. The hydroxyethylene sulfones can be traced back to four skeletons found in different aspartate protease inhibitors, as shown in Figure 2.

In comparison to the hydroxyethylene sulfone, the hydroxyethylamine core of the HIV protease inhibitor

* Corresponding author. Tel: +49 6421 282 1313. Fax: +49 6421 282 8994. E-mail: klebe@mail.uni-marburg.de.

[†] Martin-Luther-Universität Halle-Wittenberg.

[‡] Boehringer Ingelheim.

[§] Axxima Pharmaceuticals AG.

^{||} Bayer AG.

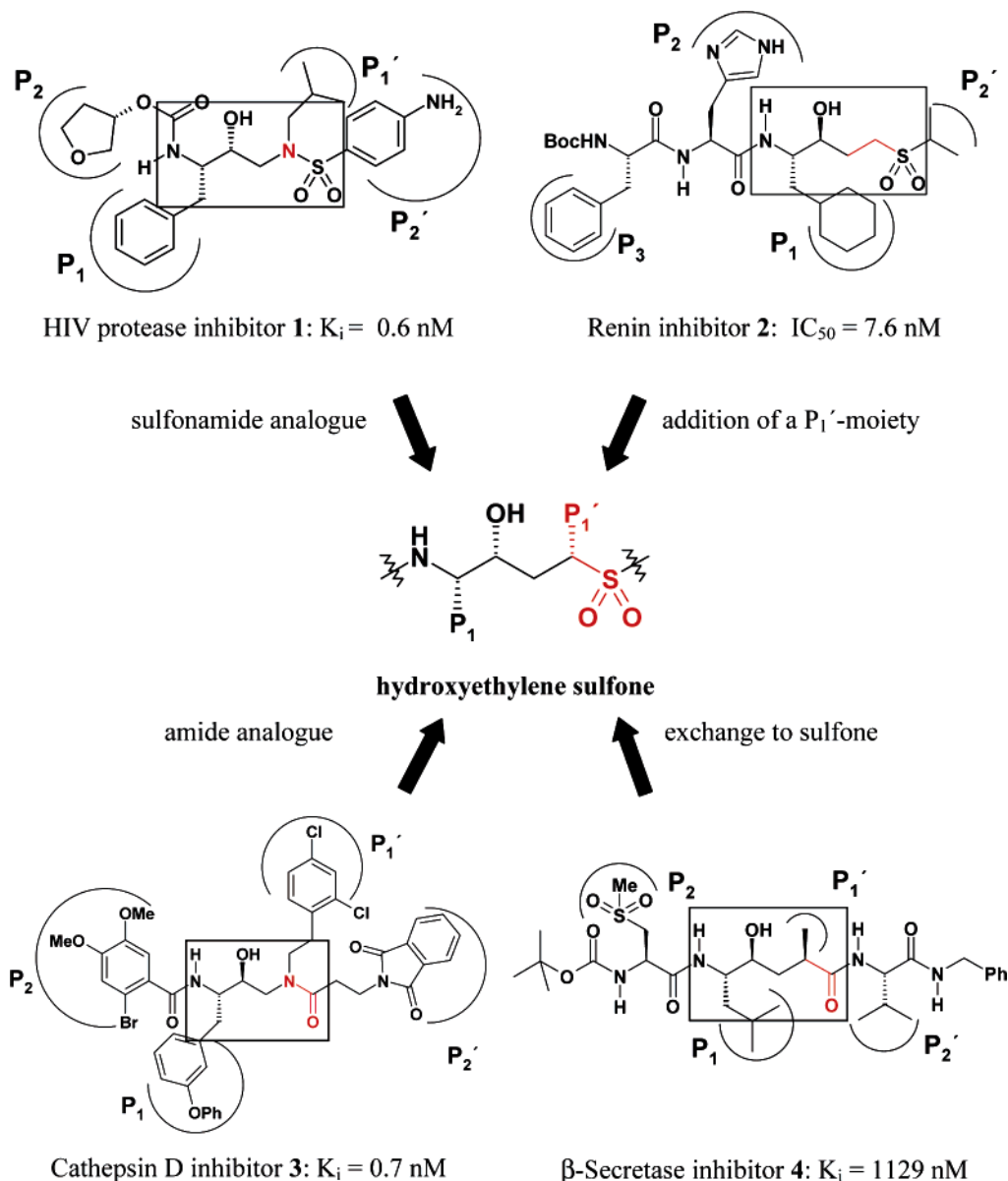


Figure 2. Analogy of hydroxyethylene sulfones with the scaffolds of four different aspartic protease inhibitors, 1–4. Functional groups of the four inhibitors, colored in red, are exchanged with a methylenesulfone moiety, highlighted in red, in the hydroxyethylene sulfone.

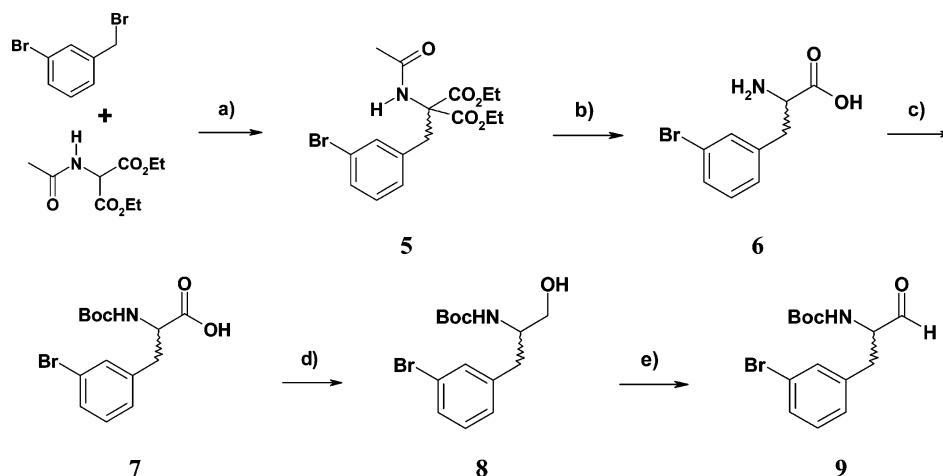
amprenavir (**1**) is altered by replacing the alkylated nitrogen atom with a carbon atom, whereas the sulfone core of the renin inhibitor **2** lacks a substitution in the α -position as the P_1 portion.^{8,9} The central scaffolds of the cathepsin D inhibitor **3** and the β -secretase inhibitor **4** are modified by replacing an amide bond or carbonyl group, respectively, with a methylenesulfone moiety in the hydroxyethylene sulfones.^{10,11}

To evaluate the viability of the hydroxyethylene sulfones as novel scaffold for aspartic acid protease inhibitors, synthetic procedures for prototype compounds have been established in which the decoration of the novel core is reminiscent of already optimized side chains found in inhibitors 1–4 (Figure 2) addressing the subsites S_2 to S_2' flanking the scissile peptide bond. A further synthetic challenge resulted from the stereochemical control of the three stereocenters contained in the hydroxyethylene sulfones. A diastereoselective synthesis is described to introduce the desired relative configuration of the stereocenters.

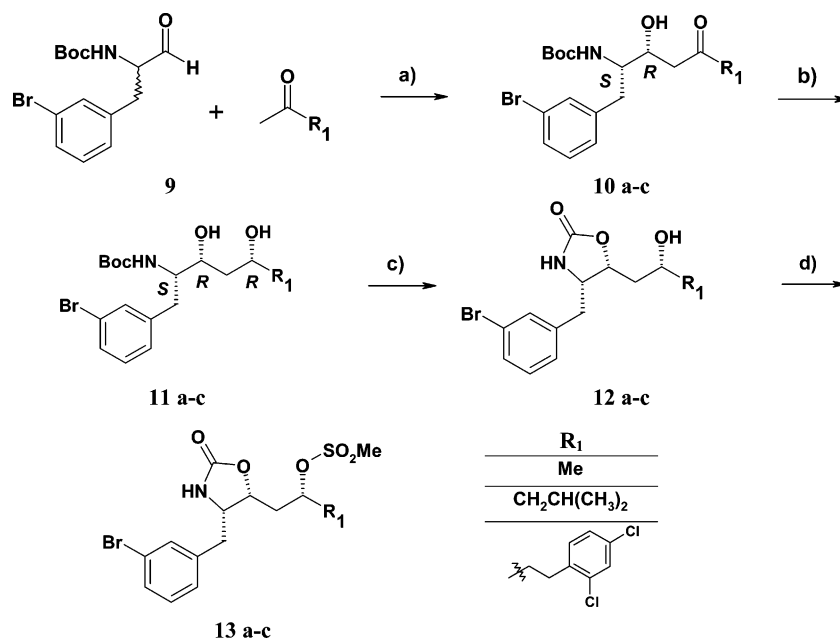
Chemistry

Scheme 1 illustrates the procedure to synthesize aldehyde **9** as a precursor to address P_1 . Reaction of 3-bromobenzyl bromide with deprotonated acetamidomalonic acid diethyl ester resulted in the formation of the substituted malonic acid diethyl ester **5**. Decarboxylation of **5** with HCl to the nonnatural amino acid **6** was followed by protection with the Boc group to **7**. *N*-Protected **7** was activated as an anhydride for the reduction with NaBH_4 to yield the primary alcohol **8**.¹² Swern oxidation afforded the racemic aldehyde **9** with an overall yield of 49%.¹³

In Scheme 2 the generation of the methanesulfonates **13a–c** is outlined. To decorate the inhibitor core fragment, shown in Figure 2 with different side chains R_1 to address the distinct S_1' subsites of the three aspartic proteases HIV protease, cathepsin D and β -secretase, three methyl ketones with distinct substitution [$R_1 =$ acetone, 4-methylpentan-2-one, 4-(2,4-dichlorophenyl)-

Scheme 1^a

^a (a) NaOEt/EtOH, (b) concd HCl, (c) (Boc)₂O, NEt₃, (d) ClCOOMe, NEt₃, NaBH₄, (e) (COCl)₂, DMSO, NEt₃.

Scheme 2^a

^a (a) LDA, -78 °C, (b) BBu₃, rt, 2 h; -78 °C, NaBH₄, (c) NaH, THF, (d) NEt₃, ClSO₂CH₃.

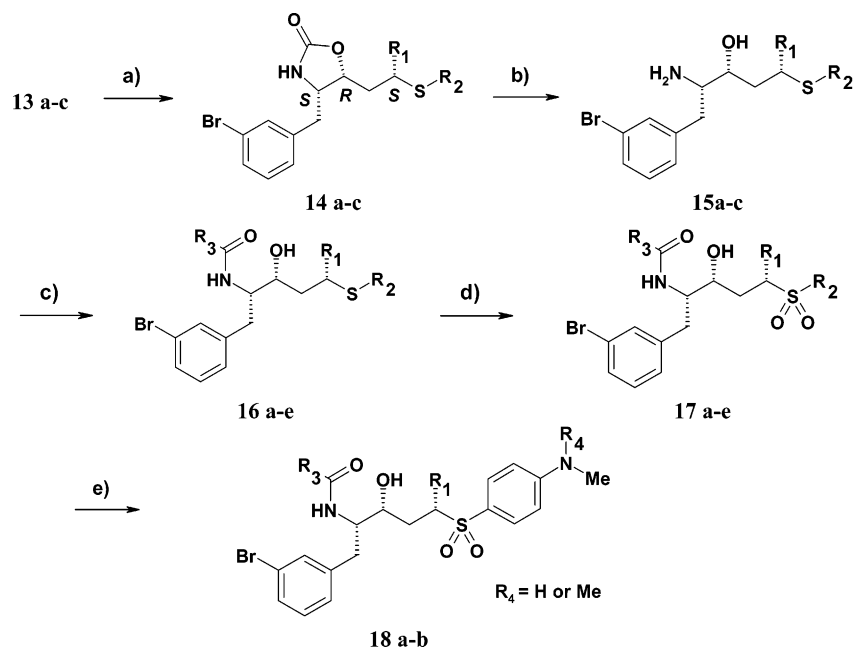
butane-2-one] were applied. The action of LDA afforded the lithiomenolates that preferentially added to the less hindered diastereotopic face of the nonchelated aldehyde carbonyl **9** to give *rac*-(*S,R*)-anti- β -hydroxy ketones **10a–c** following the model of Felkin and Anh.^{14,15} A diastereoselective 1,3 asymmetric induction has been achieved by the syn-selective reduction of **10a–c** to *rac*-(*S,R,R*)-**11a–c** 1,3-diols via boron chelates.¹⁶ Treatment with NaH proceeded via an intramolecular cyclization to oxazolidinones **12a–c** followed by mesylation to methanesulfonates **13a–c**.

The introduction of side chains to address the S₂ and S₂' subsites is described in Scheme 3. Upon treatment of **13a–c** with distinct thiolates (R₂) for addressing the S₂' subsite (3-methylbutane-1-thiolate for **13a** and 4-fluorothiophenolate for **13b–c**), S_N2 substitution took place by inversion of the configuration to thioethers **14a–c**. Cleavage of the oxazolidinone with Ba(OH)₂ led to the β -amino alcohols **15a–c**. Coupling **15a–c** with distinct carboxylic acids to **16a–e** (Table 1) for addressing the

S₂ subsite followed by oxidation of the corresponding sulfides with *m*-chloroperoxybenzoic acid (mCPBA) revealed the desired final products **17** and **18** (Table 2) with *rac*-(*S,R,S*) configuration. Introduction of one further orthogonal functionality was possible through nucleophilic substitution of the fluorine atom in **18a** and **18b** with amines or by the replacement of the aromatic bromine with palladium chemistry.

To examine whether the correct *rac*-(*S,R,S*) stereochemistry is produced, the thioether **14c** was oxidized with mCPBA to the corresponding sulfone **19** prior to the cleavage of the oxazolidinone (Figure 3). Crystal structure analysis of **19** revealed that the desired racemate was obtained.

Biological Testing of HIV-1 Protease Inhibition. Compounds **17** and **18** were tested against HIV-1 protease inhibition, because their *S*-configuration at the P₁ site and *R*-configuration at the hydroxy group are consistent with the *S,R*-configuration of the HIV-1 protease inhibitor amprenavir (**1**). Additionally, Vazquez

Scheme 3^a

^a (a) NaH, HSR₂, (b) Ba(OH)₂, (c) EDC, R₃COOH, (d) mCPBA, reflux, (e) HNMeR₄, THF, 160°C, 2 bar.

Table 1. Decorations of 16a–e

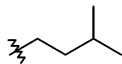
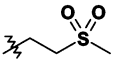
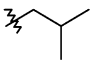
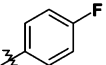
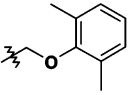
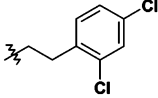
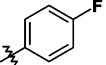
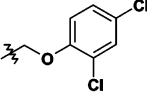
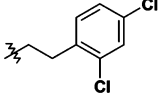
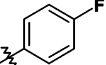
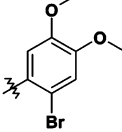
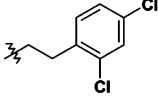
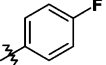
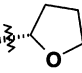
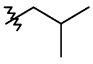
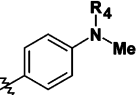
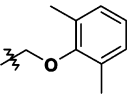
compound	R ₁	R ₂	R ₃
16 a	Me		
16 b			
16 c			
16 d			
16 e			

et al. confirmed for a series of HIV-1 protease inhibitors containing the hydroxyethylsulfonamide isostere the preference for the *S,R*-configuration of these stereocenters.¹⁷

Inhibition constants were determined using a standard assay wherein the initial rate of enzymatic cleavage of the synthetic, fluorophore-labeled substrate Abz-Thr-Ile-*p*-nitrophenylalanine-Phe-Gln-Arg-NH₂ was measured in the presence of varying concentrations of inhibitors **17** and **18**. *K_i* and IC₅₀ values are presented in Table 3.

The most potent inhibitor in the series is **17b**. It is decorated with similar side chains as the HIV-1 protease inhibitor amprenavir (**1**), addressing the S₁, S_{1'} and S_{2'} pockets of the enzyme. To replace the tetrahydrofuranyl group in **1**, the 2,6-dimethylphenoxy fragment was introduced as an achiral and specifically optimized P₂ residue for HIV-1 protease.¹⁸ The reduced affinity for **17c–e** is not surprising, since the decorations tested were originally optimized for cathepsin D. Facing the biological data of **17b** and **17c**, a drop in affinity by a factor of about 100 is indicated. We explain this differ-

Table 2. Decorations of the Hydroxyethylene Sulfones

compound	R ₁	R ₂	R ₃
17 a	Me		
17 b			
17 c			
17 d			
17 e			
18 a, b		 18 a R₄ = H 18 b R₄ = Me	

ence by the fact that the decoration of **17c** at P₁ is too large to optimally fill the S₁ pocket of the protease. The dichlorophenethyl moiety is significantly larger than any side chain found in one of the peptidic substrates recognized at the cleavage site. Nucleophilic substitution of the fluorine atom in **17b** by methylamine and dimethylamine groups provided inhibitors **18a,b**, which, however, exhibit lower affinities toward HIV-1 protease. Compound **17a**, decorated with alkyl groups, taken from the β -secretase inhibitor **4** as reference, did not show any affinity toward HIV-1 protease.

To verify whether any of the distinct stereoisomers shows deviating affinity toward HIV-1 protease, the racemic mixture of **17b** and the diastereomers of **17e** were separated via chiral HPLC. The absolute stereochemistry of the *S,R,S*-enantiomer of **17b** was determined by cocrystallization in complex with HIV-1 protease. The stereochemistry of **17e** isomers was assigned accordingly. Table 4 shows the *K_i* and IC₅₀ values of the stereochemically pure forms of **17b** and **17e**.

The results show that the enantiomer with the same *S*-configuration at P₁, as present in the natural amino acids, and the *R*-configuration at the hydroxy group (similar to the *S,R*-configuration in **1**) exhibits a significantly higher affinity compared to the *R,S*-enantiomer of **17e**. Also for the ((2*R*),1*S*,2*R*,4*S*)-stereoisomer

of **17e**, a higher affinity was observed compared to the ((2*R*),1*R*,2*S*,4*R*)-stereoisomer.

Modeling and Crystal Structure Analysis. To rationalize these observations, prior to successful crystallization and structure determination, a modeling study has been performed, using AutoDock for docking and DrugScore for scoring.^{19–22} Both enantiomers of **17b** were flexibly docked to HIV-1 protease, using the complex structure with amprenavir (**1**) (PDB code 1hpv) as reference.⁸ Docking of the *S,R,S*-enantiomer of **17b** suggested as top-ranked solution a binding mode in excellent agreement with the experimentally determined binding mode of **1**, as illustrated in Figure 4.

In contrast to the *S,R,S*-enantiomer, the *R,S,R*-enantiomer of **17b** achieved no such reasonable binding modes upon docking, properly addressing the catalytic dyad. In addition, the average docking scores for these docking solutions were significantly less favorable for the latter enantiomer. Nevertheless, the best scored docking solution exhibits a fair overlap with the side chains of amprenavir. To assess the reliability of the applied docking protocol, amprenavir (**1**) was redocked into HIV-1 protease. The top-ranked docking solution showed virtually perfect overlap with the crystallographically determined binding mode (rmsd = 0.99 Å).

After the modeling studies, we succeeded in cocrystallizing **17b** with HIV-1 protease. A racemic mixture

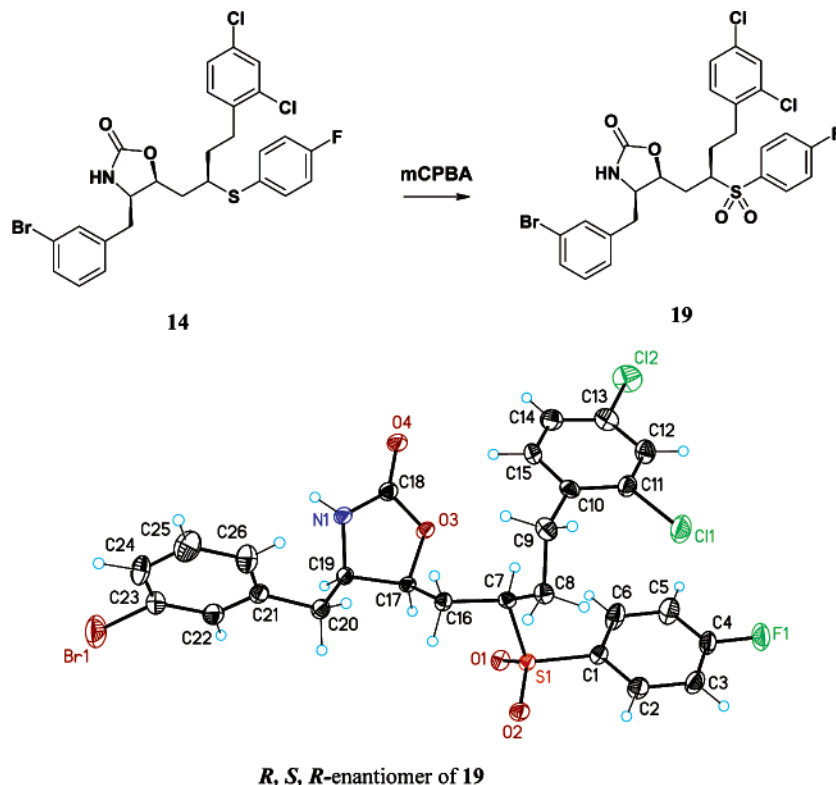


Figure 3. Crystal structure of the *R,S,R*-enantiomer of **19**.

Table 3. K_i and IC_{50} Values of Several Racemic Hydroxyethylene Sulfones for HIV-1 Protease Inhibition

compd	K_i (μ M)	IC_{50} (μ M)	compd	K_i (μ M)	IC_{50} (μ M)
17a	>40	>40	17e	3.9	5.6
17b	0.08	0.14	18a	0.37	0.53
17c	7.0	10	18b	0.54	0.79
17d	3.1	4.5			

Table 4. K_i and IC_{50} Values of Resolved Stereoisomers of **17b** and **17e** toward HIV-1 Protease

stereoisomers of 17b and 17e	K_i (μ M)	IC_{50} (μ M)
<i>S,R,S</i> - 17b	0.045	0.085
<i>R,S,R</i> - 17b	1.4	2
((2 <i>R</i>),1 <i>S</i> ,2 <i>R</i> ,4 <i>S</i>)- 17e	2.9	4.2
((2 <i>R</i>),1 <i>R</i> ,2 <i>S</i> ,4 <i>R</i>)- 17e	>40	>40

of **17b** was added to the crystallization buffer. In agreement with the predictions of modeling, the crystal structure shows that the *S,R,S*-enantiomer exhibits better binding to the protein. Exclusively, this stereoisomer is found in the binding site of HIV-1 protease (Figure 5). Figure 6 shows the superposition of *S,R,S*-**17b** with amprenavir (**1**) in the corresponding complex. Both inhibitors bind with their central hydroxy groups centered between the two aspartates, and both the carbonyl and sulfonyl groups form hydrogen bonds to the structural water which mediates interactions between bound ligand and Ile50NH or Ile50NH' in the flap region. With respect to the previously solved complex structure of amprenavir (PDB code 1hpv), the protease adopts a very similar conformation in the complex with *S,R,S*-**17b** (rmsd = 0.78 Å). No remarkable induced-fit adaptations are observed. As expected, the inhibitor occupies the four specificity pockets of the protease. Its bromobenzyl moiety is found in the S_1 pocket. It adopts

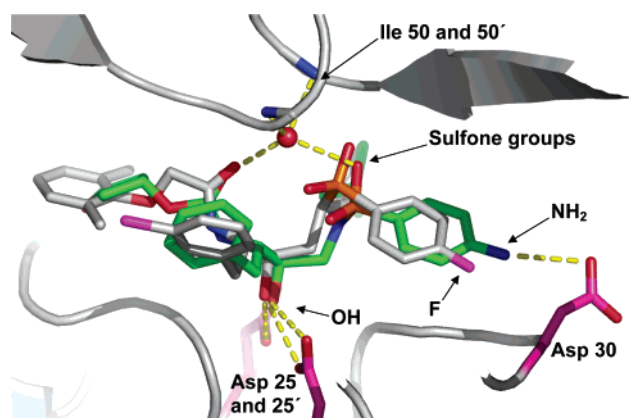


Figure 4. Predicted binding mode of *S,R,S*-**17b** in the binding pocket of HIV-1 protease, as suggested by docking. The ligand is color-coded by atom types and superimposed with the experimentally determined binding mode of amprenavir (**1**) (PDB ID 1hpv), shown in green. The protein backbone trace is schematically illustrated, and the catalytic aspartic acids and Asp30 are displayed in pink.

a nearly identical binding mode as the phenylalanine side chain in amprenavir. The additional bulky *m*-bromo substituent is oriented toward the adjacent solvent environment and thus does not provoke any induced-fit adaptations. However, in the adopted binding mode it remains partially exposed to solvent. This might be to some degree detrimental to binding affinity due to unsatisfactory burial of the hydrophobic bromo group. The S_2 pocket accommodates the *p*-fluorophenyl group of *S,R,S*-**17b**. It is found in very similar geometry as the *p*-aminophenyl group of amprenavir. Different to the latter, *S,R,S*-**17b** cannot form a similar hydrogen bond to the carboxy group of Asp30. Supposedly, this difference also contributes to the slightly reduced affinity of

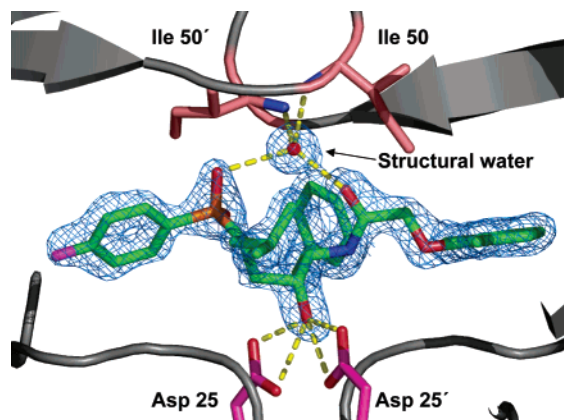


Figure 5. Crystal structure of *S,R,S*-**17b** in complex with HIV-1 protease. The protein backbone trace is schematically illustrated in gray and the catalytic aspartic acids are pink, whereas the isoleucines 50 and 50' of the flaps are displayed in salmon. The $2F_o - F_c$ density for the ligand and the structural water is displayed in blue at a σ level of 1.0.

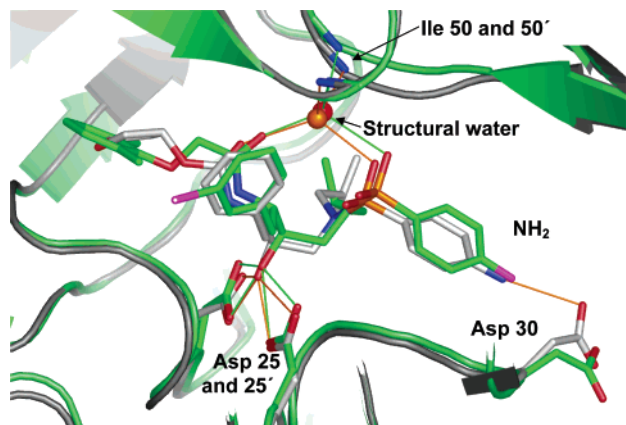


Figure 6. Crystal structure of *S,R,S*-**17b** in complex with HIV-1 protease (colored in green) superimposed with the corresponding crystal structure of amprenavir (**1**) (PDB ID 1hpv) shown in gray. The protein backbones trace, the catalytic aspartic acids, and Asp30 are illustrated in the corresponding colors.

S,R,S-**17b** compared to **1**. In both complexes the isobutyl groups of the inhibitors attached either to the amino group of **1** or to the methylenesulfone group of *S,R,S*-**17b** fill the S_1' subsite in very similar fashion. This fact explains the, on a first glance, surprising similarity of this side chain, even though attached with different stereochemistry to the ligand skeleton. The largest difference is observed for the occupancy of the S_2 pocket. While amprenavir exhibits a terminal tetrahydrofuran moiety, *S,R,S*-**17b** has been decorated by an achiral 2,6-dimethylphenoxy moiety. The latter extends deeper into this subsite and achieves nearly optimal filling of the pocket. In a direct comparison, both moieties adopt an opposing orientation in the S_2 subsite. At its far end, the dimethylphenoxy group of *S,R,S*-**17b** reaches the surrounding solvent environment.

In summary, *S,R,S*-**17b** adopts the expected binding mode. The reduced binding affinity compared to **1** possibly arises from either the unsatisfactory burial of the bromo substituent or the lack of a hydrogen bond to the carboxy group of Asp30. Further optimization of *S,R,S*-**17b** will consider these aspects in future design attempts.

Biological Evaluation for Cathepsin D and β -Secretase

Although compounds **17a** and **17c–e** were decorated with side chains that are also present in potent inhibitors of cathepsin D and β -secretase, no inhibition could be detected in cathepsin D nor in β -secretase assays. The lack of affinity might be explained by the unfavorable *S,R,S*- and *R,S,R*-configurations of the stereocenters in the hydroxyethylene sulfones for cathepsin D and β -secretase. In comparison to the more favorable *S,R*-configurations, realized in the HIV-1 protease inhibitor amprenavir **1**, Baldwin et al.²³ solved the crystal structure of cathepsin D in complex with the oligopeptide pepstatin ($K_i = 3.8$ pM). The latter inhibitor bears a statine core with *S,S*-configuration, whereas the *S,R*-stereoisomer turned out to be a much weaker inhibitor.²⁴ In addition, Lee et al.¹⁰ reported for **3** (Figure 2) that the diastereomer with the nonnatural *R*-configuration at the P_1 site together with an *S*-configuration at the hydroxy group did not inhibit cathepsin D. In contrast, the *S,S* configuration in **3** revealed inhibition with a K_i of 0.7 nM. The β -secretase inhibitor **4** and related active derivatives also possess a hydroxyethylene core solely with *S*-configuration at P_1 and *S*-configuration at the hydroxy group.¹¹

Future work will be focused on an aldole reaction with aldehyde **9** under chelate control, following methods described by Kempf or Reetz,^{25,26} to invert the stereocenters to produce the obviously more favorable *S,S*-configuration for cathepsin D and β -secretase inhibition.

Summary and Conclusion

Hydroxyethylene sulfones have been developed as a new, privileged skeleton to address the target family-wide commonality of aspartic acid proteases in substrate binding and processing. The novel motif for a transition state analogue has been derived from four different scaffolds already present in known aspartic protease inhibitors. It is ideally suited for subsequent decoration with appropriate side chain substitutions to address the structurally distinct specificity pockets in various members of the aspartic proteases family. A synthesis strategy has been established that allows stereochemical control of three stereocenters introduced into the hydroxy sulfones. The actually produced stereochemistry has been confirmed by crystal structure analysis of one final product. Enzyme kinetics revealed submicro- to micromolar inhibition of HIV protease by the racemic products. Docking of both enantiomeric forms of the most potent inhibitor suggested the *S,R,S*-enantiomer to be of higher affinity. Testing of the enantiomerically pure form separated by chromatography proves the latter enantiomer to be significantly more potent (Table 4). X-ray structure analysis of crystals prepared from a racemic mixture of the best lead compound together with HIV-1 protease confirms the stereochemistry and the binding mode suggested by docking. Even though a new stereocenter is created at the position next to the SO_2 group, the attached isobutyl substituent shows very similar occupation of the S_1' pocket. The observed reduced affinity of our best lead compound compared to amprenavir can be explained by the unsatisfactory desolvation of a hydrophobic bromo substituent in S_1 and the fact that the *p*-fluorophenyl compared to the

p-aminophenyl group in amprenavir cannot form a strong hydrogen bond to the adjacent carboxylate of Asp 30. Biological testing of the synthesized stereoisomers with respect to cathepsin D and β -secretase did not reveal satisfactory binding. Most likely, the latter proteases require inverted configuration at the hydroxy group in the portion mimicking the geometry of the transition state. Similar observations have been described for other series of aspartic protease inhibitors. This discrimination due to inverted stereochemistry at the central privileged scaffold can be exploited to achieve the desired selectivity toward different members of the aspartic protease family.

Material and Methods

Kinetic Assay. Inhibition data for HIV protease were determined as follows. IC_{50} values were taken from plots of V_i/V_0 vs inhibitor concentration, where V_i and V_0 are the catalytic rates in the presence or absence of the inhibitor. The fluorogenic substrate Abz-Thr-Ile-*p*-nitrophenylalanine-Phe-Gln-Arg-NH₂ was purchased from Bachem. To convert IC_{50} values to K_i values, the following equation was applied:

$$K_i = [IC_{50} - (E_t/2)][1 + (S/K_m)]^{-1}$$

where E_t is the total enzyme concentration (40 nM), K_m the Michaelis–Menten constant (39 μ M), and S the substrate concentration (20 μ M). Recombinant HIV-1 protease was expressed from *Escherichia coli* and purified as previously described.²⁷ Enzymatic assays were performed in 402.2 μ L assay buffer (100 mM MES, 300 mM KCl, 5 mM EDTA, 1 mg/mL BSA, pH 5.5) by addition of substrate dissolved in 8.4 μ L DMSO, and distinct inhibitor concentrations were dissolved in 8.4 μ L DMSO and 1 μ L HIV-1 protease to a final volume of 420 μ L (final DMSO concentration 4%). The hydrolysis of the substrate was recorded as an increase of the fluorescence intensity (extinction wavelength 337 nm, emission wavelength 410 nm) over a 10-min time period, during which the rate increased in a linear fashion with time.²⁸

Computational Docking. Docking was carried out using version 3.0 of the program AutoDock.^{20,21} Instead of the implemented AutoDock scoring function, DrugScore was used for calculating the required grids and for scoring, as previously described.^{19,22} The Lamarckian genetic algorithm was applied, following a standard protocol of 10 independent runs per ligand with an initial population of 50 randomly placed individuals, a maximum number of 1.5×10^6 energy evaluations, a mutation rate of 0.02, a crossover rate of 0.80, and an elitism value of 1. The probability of performing local searches on an individual in the population was 0.06, using a maximum of 300 iterations per local search.

The coordinates of HIV protease in complex with amprenavir (**1**) (PDB code 1hpv) were used as reference in docking.⁷ Ligand and solvent molecules were removed from the PDB file and DrugScore grids (16 $\text{Å} \times 14 \text{Å} \times 22 \text{Å}$, with 1 Å grid spacing) were calculated using AutoDock, as described.²² Ligand structures were constructed with Sybyl and set up for flexible docking using AutoTors, with 13 rotatable bonds for both enantiomers of **17b** and **12** for **1**.

Crystal Structure Analyses: Crystallization and Structure Determination of *S,R,S*-17b with HIV Protease. The HIV protease (7 mg/mL) in complex with the hydroxyethylene sulfone crystallizes at 18 °C in 2.7 M NaCl, 0.1 M BisTris, pH 6.5 in space group $P2_12_12_1$ (crystal data, Table 5). The crystals were obtained by cocrystallization of the enzyme with the inhibitor at 1.9 mmol/L. For cryoprotection, the crystals were briefly soaked in mother liquor containing 20% glycerol. The data set was collected at the synchrotron BESSYII in Berlin on PSF beamline I equipped with a MAR-CCD detector. In total, 221 frames with $\delta\varphi = 0.5^\circ$ at a crystal to detector distance of 120 mm were collected at -170°C . Data were processed and scaled with Denzo and Scalepack.²⁹ The struc-

Table 5. Crystal Data of *S,R,S*-17b Complexed with HIV-1 Protease

<i>S,R,S</i> -17b–HIV-1 protease	
resolution (Å)	25–1.73
space group	$P2_12_12_1$
cell dimensions (Å)	$a = 57.9$ $b = 85.8$ $c = 46.8$
highest resolution shell (Å)	1.76–1.73
no. of measured reflections	101892
no. of independent reflections	24462
completeness (%)	97.6 [79.2] ^a
I/σ	12.8 [1.7]
R_{sym} (%)	7.8 [45.2]
refined residues	198
refined ligand atoms	40
refined water molecules	207
refined chlorids	3
resolution in refinement (Å)	8–1.73
$R_{\text{cryst}} (F > 4\sigma F_o; F_o)$	16.7; 20.1
$R_{\text{free}} (F > 4\sigma F_o; F_o)$	21.0; 24.7
mean B -factor (Å ²)	17.2; 14.6
(peptide chain A; B)	
main chain (Å ²)	12.8; 11.4
side chains (Å ²)	22.1; 18.0
ligand (Å ²)	23.0
water (Å ²)	28.1
Cl ions (Å ²)	18.27
Ramachandran plot	
most favorite geometry (%)	95.6
additionally allowed (%)	4.4
generously allowed (%)	0
disallowed (%)	0

^a Values in brackets refer to the shell of highest resolution.

ture was determined by the molecular replacement method with AmoRe,³⁰ and the 1.79 Å structure of the HIV-1 protease in complex with the inhibitor Bea403 (PDB code 1ECO)³¹ was used as the search model. Refinement was continued with SHELXL-97,³² for each refinement step at least 10 cycles of conjugate gradient minimization were performed, with restraints on bond distances, angles, and B -values. Intermittent cycles of model building were done with the program O.³³ The coordinates have been deposited in the PDB (<http://www.rcsb.org/pdb/>) with access code 1XL5.

Crystal Structure Determination of **19:** $C_{26}H_{23}BrCl_2FNO_4S$, $M_r = 615.32$, monoclinic space group $C2/c$, $a = 34.013$ (2) Å , $b = 5.800$ (1) Å , $c = 26.610$ (1) Å , $\beta = 101.98$ (1) $^\circ$, $V = 5134.9$ (5) Å^3 , $Z = 8$, $d_{\text{calc}} = 1.592$ Mg m^{-3} , $F(000) = 2496$, $\lambda = 0.71073$ Å , $T = 153$ K, $\mu(\text{Mo K}\alpha) = 1.93$ mm^{-1} . Data were collected on a CAD4 diffractometer, and intensities on a cooled crystal (dimensions 0.01 \times 0.03 \times 0.4 mm) were collected at 153(2) K in the θ range 1.22–30.63 $^\circ$. Of a total of 22 554 reflections, 7835 were independent with $R_{\text{int}} = 0.077$; $R_1 = 0.043$, and $wR_2 = 0.0892$ ($I > 2\sigma(I)$), with largest difference maximum and minimum being 0.58 and -0.87 $e \text{Å}^{-3}$, respectively. Further details of the crystal structure determination are available upon request from the Cambridge Crystallographic Data Centre, 12 Union Road, Cambridge CB2 1EZ, UK, on quoting the full journal citation and the deposition number CCDC 256954.

Analytic Part. ¹H and ¹³C NMR spectra were recorded on a JEOL Eclipse + 500 instrument, using DMSO-*d*₆ or CDCl₃ with TMS as internal standard. Chemical shifts are given in ppm (δ scale). Reactions were monitored by thin-layer chromatography (TLC) on precoated Alugram SIL G/UV plates from Macherey-Nagel, and spots were visualized with UV light or with a mixture of 6 g of molybdato-phosphoric acid, 2.5 g of cerium(IV) sulfate, 470 mL of water, and 30 mL of concentrated H₂SO₄. Flash column chromatography was performed using silica gel (particle size 0.040–0.063 mm) supplied by Merck. Diethyl ether and THF were freshly distilled from LiAlH₄ under argon. Triethylamine, *N,N*-dimethylformamide (DMF), and dichloromethane were purchased from Aldrich and used without purification. High-resolution mass spectra (HRMS,

EI and ESI) were performed on either a Micromass 7070 H or a Micromass Autospec spectrometer. Analytical high performance liquid chromatography (HPLC) was carried out with a KROMASIL 100 column, type 1050 from Hewlett-Packard, C18/3.5 μm , 125.3 mm. Chiral resolution using preparative HPLC was achieved with a Semiprep HPLC of Shimadzu (column, Daicel Chiralcel OD, 30 cm length; injector, SIL-10 AD-VP). Elemental analyses were performed on a Charmomat 5-ADG from Wösthoff or HP-185. The HIV-1 protease assay was performed on a RF-5301 PC spectrofluorophotometer by Shimadzu.

Synthesis. *rac*-2-Acetylamino-2-(3-bromobenzyl)malonic Acid Diethyl Ester (5). To a solution of 2-acetylaminomalonic acid diethyl ester (86.9 g, 0.4 mol) and NaEtOAc (27.2 g, 0.4 mol) in 1.2 L of EtOH was added 1-bromo-3-bromomethylbenzene (100 g, 0.4 mol) in dropwise fashion. After being stirred under reflux for 5 h, the solution was evaporated under reduced pressure and the crude product was recrystallized in MeOH to give 113 g of **5** (75%) as a white solid. ^1H NMR (δ /ppm, 500 MHz, CDCl_3): 1.30 (t, $J = 7.1$ Hz, 6H), 2.05 (s, 3H), 3.62 (s, 2H), 4.28 (q, $J = 7.1$ Hz), 6.56 (s, 1H), 6.94 (d, $J = 7.7$ Hz, 1H), 7.14 (t, $J = 7.8$ Hz, 1H), 7.17 (m, 1H), 7.34 (d, $J = 7.7$ Hz, 1H). ^{13}C NMR (δ /ppm, 125 MHz, CDCl_3): 14.0, 23.0, 37.4, 62.8, 67.1, 122.3, 128.5, 129.8, 130.3, 132.9, 137.6, 167.3, 169.2. Anal. $\text{C}_{16}\text{H}_{20}\text{BrNO}_5$: C, H, N.

***rac*-[3-(3-Bromophenyl)-2-*tert*-butoxycarbonylamino]propionic Acid (7).** To a solution of **5** (113 g, 0.30 mol) in 900 mL of HCl was added 300 mL of acetic acid, and the reaction mixture was stirred under reflux for 16 h. The mixture was cooled to room temperature and the pH was adjusted to 6 by addition of 800 mL of NaOH. The product **6** was filtrated and dried under reduced pressure. The crude material was dissolved in 500 mL of 5% NaHCO_3 , and 67 g of Boc_2O (0.30 mol) dissolved in 300 mL of dioxane was added in one portion. After being stirred for 3 h at room temperature, the solution was acidified with 2 N HCl to a pH of 2. The reaction mixture was extracted with Et_2O (3×300 mL). The combined organic layer was dried (MgSO_4) and evaporated to give 72 g of **7** (70%) as a white foam. ^1H NMR (δ /ppm, 500 MHz, CDCl_3): 1.42 (s, 9H), 3.02 (dd, $J = 13.4, 6.7$ Hz, 1H), 3.18 (dd, $J = 13.6, 5.0$ Hz, 1H), 4.59 (m, 1H), 5.03 (d, $J = 8.0$ Hz, 1H), 7.13 (d, $J = 7.7$ Hz, 1H), 7.17 (t, $J = 7.7$ Hz, 1H), 7.34 (s, 1H), 7.39 (d, $J = 7.7$ Hz, 1H). ^{13}C NMR (δ /ppm, 125 MHz, CDCl_3): 28.3, 37.5, 54.2, 80.5, 122.5, 128.0, 130.1, 130.2, 132.5, 138.3, 155.3, 175.8. Anal. $\text{C}_{14}\text{H}_{18}\text{BrNO}_4$: C, H, N.

***rac*-[2-(3-Bromophenyl)-1-hydroxymethylethyl]carbamic Acid *tert*-Butyl Ester (8).** To a cold (-15 °C) solution of **7** (15.9 g, 69.1 mmol) in 400 mL of THF were added *N*-methylmorpholine (7.67 mL, 69.1 mmol) and isobutyl chloroformate (9.39 mL, 69.1 mmol) successively. The precipitated *N*-methylmorpholine hydrochloride was removed by filtration and washed with THF (3×50 mL). The combined organic layers were cooled to 0 °C, and sodium borohydride (3.9 g, 103 mmol) was added sequentially. The reaction mixture was quenched with 400 mL of water and extracted with EtOAc (3×100 mL). The solution was dried over MgSO_4 , filtrated, evaporated under reduced pressure, and purified by recrystallization with EtOAc to provide **8** (22.3 g, 98%) as a white solid: ^1H NMR (δ /ppm, 500 MHz, CDCl_3): 1.42 (s, 9H), 2.82 (m, 2H), 3.56 (dd, $J = 10.9, 5.0$ Hz, 1H), 3.67 (dd, $J = 11.0, 3.8$ Hz, 1H), 3.83 (m, 1H), 4.78 (d, $J = 8.1$ Hz, 1H), 7.18 (m, 2H), 7.36 (m, 2H). ^{13}C NMR (δ /ppm, 125 MHz, CDCl_3): 28.7, 37.4, 53.9, 64.4, 80.3, 122.4, 128.3, 130.1, 130.5, 132.7, 140.7, 155.1. Anal. $\text{C}_{14}\text{H}_{20}\text{BrNO}_3$: C, H, N.

***rac*-[2-(Bromophenyl)-1-formylethyl]carbamic Acid *tert*-Butyl Ester (9).** To a solution of oxalyl chloride (5.7 g, 45 mmol, 1.5 equiv) in 100 mL of CH_2Cl_2 at -78 °C was added 7.02 g DMSO (90 mmol, 3 equiv) under argon in a dropwise fashion. The reaction mixture was stirred for 30 min by dropwise addition of **8** (10 g, 300 mmol) solved in 400 mL of CH_2Cl_2 . The reaction was kept at -78 °C for 30 min, and TEA (23.3 g, 0.18 mol, 6 equiv) was added subsequently. The reaction was allowed to warm to room temperature and washed sequentially with 1 N HCl, saturated NaHCO_3 , and

brine. The organic layer was dried (MgSO_4), filtered, and concentrated. Column chromatography (cyclohexane/EtOAc 3:1) of the residue provided 9.59 g (29 mmol, 96%) of **9** as a white solid: ^1H NMR (δ /ppm, 500 MHz, CDCl_3): 1.45 (s, 9H), 3.05 (dd, $J = 14.1, 6.7$ Hz, 2H), 3.14 (dd, $J = 14.1, 6.4$ Hz, 2H), 4.39 (m, 1H), 5.08 (d, $J = 5.6$ Hz, 1H), 7.10 (d, $J = 7.7$ Hz, 1H), 7.19 (t, $J = 7.8$ Hz, 1H), 7.33 (s, 1H), 7.64 (d, $J = 7.8$ Hz, 1H). ^{13}C NMR (δ /ppm, 125 MHz, CDCl_3): 28.6, 35.3, 61.0, 80.8, 123.1, 128.3, 130.6, 130.6, 132.8, 138.6, 155.6, 199.1. Anal. $\text{C}_{14}\text{H}_{18}\text{BrNO}_3$: C, H, N.

***rac*-(1*S*,2*R*)-[1-(Bromobenzyl)-2-hydroxy-4-oxopentyl]carbamic Acid *tert*-Butyl Ester (10a).** To a solution of LDA (54 mL, 1 M in THF) in 100 mL of anhydrous THF at -78 °C was added acetone (1.22 g, 21 mmol) dropwise. After being stirred for 30 min at -78 °C, the solution was treated by dropwise addition of **9** (6.9 g, 21 mmol) solved in 200 mL of THF at -78 °C. The reaction mixture was warmed to room temperature and quenched with 300 mL of saturated NH_4Cl . The solution was extracted with CH_2Cl_2 (3×100 mL), dried over MgSO_4 , and evaporated under reduced pressure. The diastereomeric mixture (de = 92:8 determined by HPLC) could be purified by column chromatography (cyclohexane/EtOAc 1:1) to give the *rac*-(*S,R*)-isomers of **10a** (4.25 g, 52%). ^1H NMR (δ /ppm, 500 MHz, $\text{DMSO}-d_6$): 1.39 (m, 9H), 2.01 (s, 3H), 2.50 (m, 3H), 3.01 (dd, $J = 13.7, 3.2$ Hz, 1H), 3.45 (m, 1H), 3.82 (m, 1H), 4.98 (d, $J = 6.6$ Hz, 1H), 6.65 (d, $J = 9.6$ Hz, 1H) 7.19 (m, 2H), 7.33 (d, $J = 3.3$ Hz, 1H), 7.38 (s, 1H). ^{13}C NMR (δ /ppm, 125 MHz, $\text{DMSO}-d_6$): 28.7, 31.1, 36.3, 48.8, 57.2, 70.3, 78.1, 121.8, 128.2, 128.4, 129.8, 131.8, 143.8, 155.8, 208.1. Anal. $\text{C}_{17}\text{H}_{24}\text{BrNO}_4$: C, H, N.

***rac*-(1*S*,2*R*)-[1-(Bromobenzyl)-2-hydroxy-6-methyl-4-oxoheptyl]carbamic Acid *tert*-Butyl Ester (10b)** was prepared analogously to **10a** using 4-methylpentan-2-one as alkyl methyl ketone (2.1 g, 21 mmol) with 57% yield (de = 94:6). ^1H NMR (δ /ppm, 500 MHz, $\text{DMSO}-d_6$): 0.86 (d, $J = 6.7$ Hz, 6H), 1.22 (m, 9H), 1.98 (m, 1H), 2.28 (m, 2H), 2.47 (m, 3H), 2.98 (dd, $J = 13.9, 3.2$ Hz, 1H), 3.42 (m, 1H), 3.79 (m, 1H), 5.03 (d, $J = 6.7$ Hz, 1H), 6.64 (d, $J = 9.6$ Hz, 1H), 7.19 (m, 2H), 7.32 (m, 1H), 7.37 (s, 1H). ^{13}C NMR (δ /ppm, 125 MHz, $\text{DMSO}-d_6$): 22.3, 23.6, 28.1, 35.6, 47.6, 51.6, 56.5, 69.6, 77.4, 121.2, 128.2, 128.4, 129.8, 131.8, 142.5, 155.2, 209.0. Anal. $\text{C}_{20}\text{H}_{30}\text{BrNO}_4$: C, H, N.

***rac*-(1*S*,2*R*)-[1-(Bromobenzyl)-6-[2,4-dichlorophenyl]-2-hydroxy-4-oxohexyl]carbamic Acid *tert*-Butyl Ester (10c)** was synthesized following the above procedure in analogy to **10a** by addition of 4-(2,4-dichlorophenyl)butan-2-one (4.55 g, 21 mmol) in 80% yield (de = 94:6). ^1H NMR (δ /ppm, 500 MHz, CDCl_3): 1.25 (s, 9H), 2.51 (m, 3H), 2.78 (m, 2H), 2.85 (m, 2H), 3.00 (m, 1H), 3.45 (m, 1H), 3.83 (m, 1H), 5.06 (d, $J = 6.6$ Hz, 1H), 6.69 (d, $J = 9.5$ Hz, 1H), 7.20 (m, 2H), 7.36 (m, 4H), 7.57 (s, 1H). ^{13}C NMR (δ /ppm, 125 MHz, CDCl_3): 26.1, 28.0, 35.6, 41.8, 47.3, 56.6, 69.7, 77.4, 121.4, 127.2, 128.2, 128.4, 128.4, 129.9, 131.3, 131.7, 131.8, 133.7, 137.6, 142.4, 155.2, 208.1. Anal. $\text{C}_{24}\text{H}_{28}\text{BrCl}_2\text{NO}_4$: C, H, N.

***rac*-(1*S*,2*R*,4*R*)-[1-(3-Bromobenzyl)-2,4-dihydroxypentyl]carbamic Acid *tert*-Butyl Ester (11a).** A THF (200 mL) solution of tributylborane (2 g, 11 mmol) and **10a** (3.86 g, 10 mmol) was stirred for 2 h at room temperature under argon atmosphere. Subsequently, the solution was cooled to -78 °C, and solid NaBH_4 (440 mg, 11 mmol) was added in one portion. It was essential for the asymmetric reduction to stir the reaction mixture at -78 °C for at least 7 h. The solution was quenched with a mixture of 30% H_2O_2 (50 mL), $\text{Na}_2\text{HPO}_4/\text{NaH}_2\text{PO}_4$ buffer (pH 7, 100 mL), and MeOH (150 mL). The organic solvent was evaporated under reduced pressure and the residual solution was extracted with CH_2Cl_2 (3×100 mL). The combined organic layers were dried over MgSO_4 and condensed in vacuo. To decompose the remaining boronic acid ester, 40 mL of 1% HCl in MeOH was added, and the solution was stirred at room temperature overnight, evaporated (de = 99:1 determined by HPLC), and flash chromatographed on silica gel (cyclohexane/EtOAc 1:1) to give *rac*-(*S,R,R*)-**11a** (2.87 g, 74%). ^1H NMR (δ /ppm, 500 MHz, $\text{DMSO}-d_6$): 1.06 (d, $J = 6.1$ Hz, 3H), 1.29 (m, 9H), 1.49 (m, 1H), 2.50 (m, 1H), 2.99

(dd, $J = 13.9, 2.0$ Hz, 1H), 3.48 (m, 2H), 3.82 (m, 1H), 4.53 (d, $J = 4.1$ Hz, 1H), 4.78 (d, $J = 4.8$ Hz, 1H), 6.58 (d, $J = 8.7$ Hz, 1H), 7.19 (m, 2H), 7.34 (d, $J = 3.3$ Hz, 1H), 7.38 (s, 1H). ^{13}C NMR (δ/ppm , 125 MHz, DMSO- d_6): 23.3, 28.1, 35.5, 42.6, 56.6, 64.9, 71.5, 77.3, 121.2, 128.2, 128.4, 129.8, 131.8, 142.7, 155.2. HRMS (ESI) m/z : $\text{C}_{17}\text{H}_{27}\text{BrNO}_4$ (MH^+) calcd, 388.1123, found, 388.1143.

***rac*-(1*S*,2*R*,4*R*)-[1-(3-Bromobenzyl)-2,4-dihydroxy-6-methylheptyl]carbamic Acid *tert*-Butyl Ester (11b)** was obtained in same manner as 11a with 70% yield (de = 99:1). ^1H NMR (δ/ppm , 500 MHz, DMSO- d_6): 0.86 (m, 6H), 1.24 (m, 2H), 1.24 (m, 9H), 1.36 (m, 1H), 1.39 (m, 1H), 1.75 (m, 1H), 2.50 (m, 1H), 2.98 (dd, $J = 13.8, 3.1$ Hz, 1H), 3.47 (m, 1H), 3.47 (m, 1H), 3.68 (m, 1H), 4.46 (d, $J = 5.0$ Hz, 1H), 4.83 (d, $J = 4.6$ Hz, 1H), 6.58 (d, $J = 9.1$ Hz, 1H), 7.20 (m, 2H), 7.32 (m, 1H), 7.38 (s, 1H). ^{13}C NMR (δ/ppm , 125 MHz, DMSO- d_6): 21.9, 23.5, 23.8, 28.1, 35.3, 41.5, 46.4, 56.5, 67.1, 71.7, 77.3, 121.1, 128.2, 128.3, 129.8, 131.8, 142.9, 155.2. Anal. $\text{C}_{20}\text{H}_{32}\text{BrNO}_4$: C, H, N.

***rac*-(1*S*,2*R*,4*R*)-[1-(3-Bromobenzyl)-6-(2,4-dichlorophenyl)-2,4-dihydroxyhexyl]carbamic Acid *tert*-Butyl Ester (11c)** was prepared in same manner as 11a with 76% yield (de = 99:1). ^1H NMR (δ/ppm , 500 MHz, DMSO- d_6): 1.26 (s, 9H), 1.52 (m, 2H), 1.65 (m, 2H), 2.50 (m, 1H), 2.67 (m, 1H), 2.80 (m, 1H), 2.97 (m, 1H), 3.44 (m, 2H), 3.68 (m, 1H), 4.70 (d, $J = 4.6$ Hz, 1H), 4.85 (d, $J = 5.2$ Hz, 1H), 6.63 (d, $J = 8.9$ Hz), 7.19 (m, 2H), 7.35 (m, 4H), 7.55 (s, 1H). ^{13}C NMR (δ/ppm , 125 MHz, DMSO- d_6): 28.0, 28.4, 35.3, 36.3, 40.8, 56.6, 66.0, 67.9, 77.3, 121.1, 127.2, 128.2, 128.4, 128.5, 129.9, 131.0, 131.7, 131.8, 133.7, 139.0, 142.6, 155.1. HRMS (ESI) m/z : $\text{C}_{24}\text{H}_{30}\text{BrCl}_2\text{NO}_4 + \text{Na}^+$ calcd, 568.0627; found, 568.0624. Anal. $\text{C}_{24}\text{H}_{30}\text{BrCl}_2\text{NO}_4$: C, H, N.

***rac*-(4*S*,5*R*,2*R*)-4-(3-Bromobenzyl)-5-(2-hydroxypropyl)-1,3-oxazolidin-2-one (12a)**. To a mixture of NaH (0.5 g, 20.7 mmol) in 50 mL of THF was added a solution of 11a (2.68 g, 6.9 mmol) in 50 mL of THF in a dropwise fashion. The reaction mixture was stirred at room temperature for 2 h and poured into a saturated solution of NH_4Cl (100 mL). The aqueous layer was extracted with Et_2O (3×50 mL), and the combined extracts were washed with brine (3×50 mL). The organic layer was dried (MgSO_4), filtered, and concentrated in vacuo. Flash chromatography (cyclohexane/EtOAc 1:1) afforded 12a (1.41 g, 66% yield) as a white solid: ^1H NMR (δ/ppm , 500 MHz, DMSO- d_6): 1.08 (d, $J = 6.2$ Hz, 3H), 1.66 (ddd, $J = 14.0, 6.5, 5.0$ Hz, 1H), 1.84 (ddd, $J = 13.9, 8.7, 5.7$ Hz, 1H), 2.58 (dd, $J = 12.9, 9.1$ Hz, 1H), 2.87 (dd, $J = 13.7, 4.6$ Hz, 1H), 4.60 (d, $J = 4.8$ Hz, 1H), 4.03 (m, 1H), 4.64 (m, 1H), 7.26 (m, 2H), 7.41 (m, 1H), 7.49 (s, 1H), 7.57 (s, 1H). ^{13}C NMR (δ/ppm , 125 MHz, DMSO- d_6): 22.8, 35.6, 35.6, 38.1, 55.3, 63.1, 76.4, 121.6, 128.2, 129.1, 130.4, 131.8, 140.6, 157.9. Anal. $\text{C}_{13}\text{H}_{16}\text{BrNO}_3$: C, H, N.

***rac*-(4*S*,5*R*,2*R*)-4-(3-Bromobenzyl)-5-(2-hydroxy-4-methylpentyl)-1,3-oxazolidin-2-one (12b)** was obtained in the same manner as 12a with 67% yield. ^1H NMR (δ/ppm , 500 MHz, DMSO- d_6): 0.81 (d, $J = 6.8$ Hz, 3H), 0.86 (d, $J = 6.8$ Hz, 3H), 1.14 (m, 1H), 1.26 (m, 1H), 1.75 (m, 1H), 1.75 (m, 2H), 2.58 (dd, $J = 14.0, 5.0$ Hz, 1H), 2.84 (dd, $J = 13.8, 8.9$ Hz, 1H), 3.52 (m, 1H), 4.05 (m, 1H), 4.47 (d, $J = 5.8$ Hz, 1H), 4.67 (m, 1H), 7.25 (m, 2H), 7.41 (m, 1H), 7.47 (s, 1H), 7.56 (s, 1H). ^{13}C NMR (δ/ppm , 125 MHz, DMSO- d_6): 21.7, 23.6, 23.8, 35.6, 37.6, 45.7, 55.3, 64.8, 78.6, 121.6, 128.2, 129.1, 130.4, 131.8, 140.6, 158.0. HRMS (ESI) m/z : $\text{C}_{16}\text{H}_{22}\text{BrNO}_3 + \text{Na}^+$ calcd, 378.0681; found, 378.0677. Anal. $\text{C}_{16}\text{H}_{22}\text{BrNO}_3$: C, H, N.

***rac*-(4*S*,5*R*,2*R*)-4-(3-Bromobenzyl)-5-[4-(2,4-dichlorophenyl)-2-hydroxybutyl]-1,3-oxazolidin-2-one (12c)** was prepared analogously to 12a with 64% yield. ^1H NMR (δ/ppm , 500 MHz, DMSO- d_6): 1.58 (m, 1H), 1.68 (m, 1H), 1.82 (m, 2H), 2.62 (m, 2H), 2.84 (m, 2H), 3.55 (m, 1H), 4.06 (m, 1H), 4.73 (m, 1H), 4.80 (s, 1H), 7.26 (m, 2H), 7.36 (m, 2H), 7.42 (m, 1H), 7.47 (s, 1H), 7.55 (s, 1H), 7.61 (s, 1H). ^{13}C NMR (δ/ppm , 125 MHz, DMSO- d_6): 28.8, 35.6, 36.2, 36.5, 55.4, 66.4, 76.4, 121.8, 127.4, 128.4, 128.7, 129.3, 130.6, 131.3, 132.0, 132.0, 133.9, 139.0, 140.8, 158.2. Anal. $\text{C}_{20}\text{H}_{20}\text{BrCl}_2\text{NO}_3$: C, H, N.

***rac*-(4*S*,5*R*,1*R*)-Methanesulfonic Acid 2-[4-(3-Bromobenzyl)-2-oxooxazolidin-5-yl]-1-methylethyl Ester (13a)**. A solution of 12a (1.39 g, 3.9 mmol) and triethylamine (2.36 g, 23.4 mmol) in 200 mL of CH_2Cl_2 was cooled to 0°C and treated by dropwise addition of mesyl chloride (1.32 g, 11.7 mmol). After being stirred for 2 h at 0°C , the solution was quenched with 0.5 N HCl (3×50 mL) and washed with NaHCO_3 (3×50 mL) and brine solution (3×50 mL). The organic solution was dried (MgSO_4), evaporated, and flash chromatographed (cyclohexane/EtOAc 1:1) to give 1.3 g (84%) of 13a as a white powder. ^1H NMR (δ/ppm , 500 MHz, DMSO- d_6): 1.39 (d, $J = 6.5$ Hz, 3H), 1.99 (m, 1H), 2.15 (m, 1H), 2.60 (dd, $J = 13.6, 10.0$ Hz, 1H), 2.90 (dd, $J = 13.8, 4.3$ Hz, 1H), 3.18 (s, 3H), 4.05 (m, 1H), 4.71 (ddd, $J = 10.5, 6.7, 3.8$ Hz, 1H), 4.81 (m, 1H), 7.26 (m, 2H), 7.43 (m, 1H), 7.52 (s, 1H), 7.66 (s, 1H). ^{13}C NMR (δ/ppm , 125 MHz, DMSO- d_6): 20.3, 31.7, 35.4, 37.8, 55.2, 75.2, 76.9, 121.6, 128.2, 129.1, 130.4, 131.8, 140.5, 157.5. Anal. $\text{C}_{14}\text{H}_{18}\text{BrNO}_5\text{S}$: C, H, N.

***rac*-(4*S*,5*R*,3*R*)-Methanesulfonic Acid 1-[4-(3-Bromobenzyl)-2-oxooxazolidin-5-ylmethyl]-3-methylbutyl Ester (13b)** was prepared from 12b in the same manner as 13a with yield of 80%. ^1H NMR (δ/ppm , 500 MHz, DMSO- d_6): 0.90 (d, $J = 6.6$ Hz, 6H), 1.51 (ddd, $J = 13.1, 7.3, 3.0$ Hz, 1H), 1.60 (ddd, $J = 14.2, 8.6, 4.9$ Hz, 1H), 1.72 (m, 1H), 2.05 (ddd, $J = 14.3, 6.9, 3.1$ Hz, 1H), 2.16 (ddd, $J = 14.9, 10.3, 4.9$ Hz, 1H), 2.63 (dd, $J = 13.7, 9.2$ Hz, 1H), 2.88 (dd, $J = 13.9, 4.8$ Hz, 1H), 3.18 (s, 3H), 4.08 (m, 1H), 4.72 (ddd, $J = 10.2, 7.4, 3.0$ Hz, 1H), 4.80 (m, 1H), 7.25 (m, 2H), 7.42 (m, 1H), 7.47 (s, 1H), 7.68 (s, 1H). ^{13}C NMR (δ/ppm , 125 MHz, DMSO- d_6): 21.6, 22.9, 23.6, 31.5, 34.2, 35.3, 44.6, 55.3, 75.3, 79.1, 121.5, 128.2, 129.2, 130.4, 131.8, 140.4, 157.6. HRMS (ESI) m/z : $\text{C}_{17}\text{H}_{24}\text{BrNO}_5\text{S} + \text{Na}^+$ calcd, 456.0456; found, 456.0494. Anal. $\text{C}_{17}\text{H}_{24}\text{BrNO}_5\text{S}$: C, H, N.

***rac*-(4*S*,5*R*,3*R*)-Methanesulfonic Acid 1-[4-(3-Bromobenzyl)-2-oxooxazolidin-5-ylmethyl]-3-(2,4-dichlorophenyl)propyl Ester (13c)** was obtained from 12c in the same manner as 12a with 82% yield. ^1H NMR (δ/ppm , 500 MHz, DMSO- d_6): 1.92 (m, 1H), 2.01 (m, 1H), 2.15 (ddd, $J = 14.8, 6.8, 3.3$ Hz, 1H), 2.22 (ddd, $J = 14.6, 9.8, 5.3$ Hz, 1H), 2.65 (dd, $J = 13.7, 9.5$ Hz, 1H), 2.80 (m, 2H), 2.91 (dd, $J = 13.7, 4.5$ Hz, 1H), 3.22 (s, 3H), 4.11 (m, 1H), 4.76 (m, 1H), 4.85 (m, 1H), 7.28 (m, 2H), 7.42 (m, 3H), 7.49 (s, 1H), 7.59 (s, 1H), 7.72 (s, 1H). ^{13}C NMR (δ/ppm , 125 MHz, DMSO- d_6): 27.6, 31.4, 33.2, 35.3, 37.9, 55.2, 75.1, 79.5, 121.7, 127.4, 128.2, 128.6, 129.2, 130.4, 131.5, 131.8, 131.8, 133.7, 137.6, 140.4, 157.6. Anal. $\text{C}_{21}\text{H}_{22}\text{BrCl}_2\text{NO}_5\text{S}$: C, H, N.

***rac*-(4*S*,5*R*,2*S*)-4-(3-Bromobenzyl)-5-[2-(3-methylbutylsulfanyl)propyl]-1,3-oxazolidin-2-one (14a)**. To a 0°C solution of NaH (65 mg, 2.7 mmol) in 50 mL of THF was added 3-methyl-butane-1-thiol (281 mg, 2.7 mmol) in one portion. The mixture was treated by dropwise addition of 13a dissolved in 20 mL of THF. The reaction mixture was stirred for 1 h at room temperature and then distributed between 35 mL of CH_2Cl_2 and 35 mL of brine. The organic layer was dried with MgSO_4 and evaporated. The residue was chromatographed on silica gel eluting with cyclohexane/EtOAc (2:1) to give 880 mg (83%) of 14a. ^1H NMR (δ/ppm , 500 MHz, DMSO- d_6): 0.86 (d, $J = 1.0$ Hz, 3H), 0.88 (d, $J = 1.2$ Hz, 3H), 1.32 (d, $J = 6.9$ Hz, 3H), 1.38 (m, 2H), 1.63 (m, 1H), 1.68 (ddd, $J = 14.6, 9.7, 3.0$ Hz, 1H), 2.15 (ddd, $J = 14.9, 10.4, 4.4$ Hz, 1H), 2.49 (m, 2H), 2.63 (dd, $J = 13.8, 9.1$ Hz, 1H), 2.82 (m, 1H), 2.89 (dd, $J = 13.9, 4.9$ Hz, 1H), 4.14 (m, 1H), 4.80 (ddd, $J = 10.4, 7.8, 3.4$ Hz, 1H), 7.26 (m, 2H), 7.41 (m, 1H), 7.47 (s, 1H), 7.59 (s, 1H). ^{13}C NMR (δ/ppm , 125 MHz, DMSO- d_6): 21.9, 22.5, 27.6, 27.7, 35.2, 36.5, 36.7, 38.2, 54.9, 76.7, 121.5, 127.9, 128.8, 130.2, 132.1, 140.4, 157.3. HRMS (ESI) m/z : $\text{C}_{18}\text{H}_{27}\text{BrNO}_2\text{S}$ (MH^+) calcd, 400.0964; found, 400.0945. Anal. $\text{C}_{18}\text{H}_{26}\text{BrNO}_2\text{S}$: C, H, N.

***rac*-(4*S*,5*R*,2*S*)-4-(3-Bromobenzyl)-5-[2-(4-fluorophenylsulfanyl)-4-methylpentyl]-1,3-oxazolidin-2-one (14b)** was synthesized following the above procedure by addition of 4-fluorobenzenethiol (346 mg, 2.7 mmol) and 13b with 80% yield. ^1H NMR (δ/ppm , 500 MHz, DMSO- d_6): 0.82 (d, $J = 3.0$ Hz, 3H), 0.84 (d, $J = 3.2$ Hz, 3H), 1.37 (m, 2H), 1.53 (ddd, $J =$

14.7, 10.5, 2.0 Hz, 1H), 1.88 (m, 1H), 1.95 (ddd, $J = 14.7, 11.5, 3.4$ Hz, 1H), 2.64 (dd, $J = 14.0, 8.8$ Hz, 1H), 2.83 (dd, $J = 14.0, 5.3$ Hz, 1H), 3.06 (m, 1H), 4.20 (m, 1H), 4.99 (ddd, $J = 11.7, 7.8, 2.0$ Hz, 1H), 7.20 (m, 4H), 7.40 (m, 4H), 7.65 (s, 1H). ^{13}C NMR (δ/ppm , 125 MHz, DMSO- d_6): 22.1, 22.3, 24.8, 34.3, 35.3, 44.5, 44.7, 57.8, 76.3, 116.1, 121.5, 128.0, 128.3, 129.1, 130.4, 131.8, 135.5, 140.5, 157.8, 161.7. HRMS (ESI) m/z : $\text{C}_{22}\text{H}_{26}\text{BrFNO}_2\text{S}$ (MH^+) calcd, 466.0852; found, 466.0885. Anal. $\text{C}_{22}\text{H}_{25}\text{BrFNO}_2\text{S}$: C, H, N.

rac-(4S,5R,2S)-4-(3-Bromobenzyl)-5-[4-(2,4-dichlorophenyl)-2-(4-fluorophenylsulfanyl)butyl]-1,3-oxazolidin-2-one (14c) was produced following the above procedure by addition of 4-fluorobenzenethiol (346 mg, 2.7 mmol) and **13c** in 80% yield. ^1H NMR (δ/ppm , 500 MHz, DMSO- d_6): 1.65 (m, 1H), 1.79 (m, 2H), 2.08 (m, 1H), 2.67 (m, 1H), 2.87 (m, 3H), 3.17 (m, 1H), 4.21 (m, 1H), 4.99 (m, 1H), 7.18 (m, 2H), 7.28 (m, 2H), 7.36 (m, 2H), 7.43 (s, 3H), 7.48 (s, 1H), 7.55 (s, 1H), 7.70 (s, 1H). ^{13}C NMR (δ/ppm , 125 MHz, DMSO- d_6): 29.8, 34.1, 35.3, 35.7, 46.5, 55.3, 76.7, 116.5, 122.1, 127.8, 128.5, 128.7, 129.0, 129.6, 130.8, 131.8, 132.1, 132.4, 134.1, 135.6, 138.4, 141.0, 158.1, 162.1. Anal. $\text{C}_{26}\text{H}_{23}\text{BrCl}_2\text{FNO}_2\text{S}$: C, H, N.

rac-(2S,3R,5S)-2-Amino-1-(3-bromophenyl)-5-(3-methylbutylsulfanyl)hexan-3-ol (15a). A solution of **14a** (0.8 g, 2 mmol) and barium hydroxide octahydrate (1.1 g, 4 mmol) in dioxane (100 mL) and water (60 mL) was heated at reflux under N_2 overnight. The solid barium carbonate was filtered and the filtrate was diluted with water. The resulting solution was extracted with Et_2O (3×50 mL), and the combined organic extracts were washed with brine, dried over MgSO_4 , and evaporated to a residue. Flash chromatography on silica gel eluting with EtOAc gave 560 mg (75%) of **15a**. ^1H NMR (δ/ppm , 500 MHz, DMSO- d_6): 0.86 (d, $J = 0.8$ Hz, 3H), 0.88 (d, $J = 0.9$ Hz, 3H), 1.24 (d, $J = 6.7$ Hz, 3H), 1.40 (m, 2H), 1.47 (m, 1H), 1.64 (m, 2H), 2.36 (dd, $J = 12.8, 7.8$ Hz, 1H), 2.49 (m, 2H), 2.74 (m, 2H), 2.93 (m, 1H), 3.27 (s, 2H), 4.48 (m, $J = 5.7$ Hz, 1H), 7.23 (m, 2H), 7.37 (m, 1H), 7.44 (s, 1H). ^{13}C NMR (δ/ppm , 125 MHz, DMSO- d_6): 21.9, 23.0, 26.7, 26.8, 38.5, 39.0, 39.1, 39.2, 57.5, 71.7, 121.4, 128.1, 128.3, 129.9, 131.7, 143.3. HRMS (ESI) m/z : $\text{C}_{17}\text{H}_{29}\text{BrNOS}$ (MH^+) calcd, 374.1181; found, 374.1153.

rac-(2S,3R,5S)-2-Amino-1-(3-bromophenyl)-5-(4-fluorophenylsulfanyl)-7-methyloctan-3-ol (15b) was synthesized from **14b** as described for **15a** with 72% yield. ^1H NMR (δ/ppm , 500 MHz, DMSO- d_6): 0.81 (d, $J = 6.7$ Hz, 3H), 0.83 (d, $J = 6.7$ Hz, 3H), 1.37 (m, 2H), 1.58 (m, 2H), 1.81 (m, 1H), 2.35 (dd, $J = 12.9, 9.4$ Hz, 1H), 2.73 (m, 1H), 2.97 (dd, $J = 13.4, 4.3$ Hz, 1H), 3.27 (m, 1H), 3.67 (m, 1H), 4.68 (d, $J = 6.1$ Hz, 1H), 7.20 (m, 4H), 7.40 (m, 4H). ^{13}C NMR (δ/ppm , 125 MHz, DMSO- d_6): 22.1, 22.3, 24.8, 37.3, 38.9, 44.5, 45.6, 57.7, 71.3, 116.5, 121.3, 128.3, 128.4, 128.7, 129.9, 130.0, 131.8, 134.7, 142.3, 161.4. Anal. $\text{C}_{21}\text{H}_{27}\text{BrFNO}_3$: C, H, N.

rac-(2S,3R,5S)-2-Amino-1-(3-bromophenyl)-7-(2,4-dichlorophenyl)-5-(4-fluorophenylsulfanyl)heptan-3-ol (15c) was obtained from **14c** in the same manner as **15a** with 80% yield. ^1H NMR (δ/ppm , 500 MHz, DMSO- d_6): 1.70 (m, 2H), 1.80 (m, 1H), 2.39 (dd, $J = 12.9, 8.9$ Hz, 1H), 2.78 (m, 2H), 2.84 (m, 2H), 3.34 (m, 1H), 3.57 (m, 1H), 4.63 (d, $J = 5.72$ Hz, 1H), 7.14 (m, 2H), 7.24 (m, 2H), 7.31 (m, 2H), 7.37 (m, 2H), 7.46 (m, 2H), 7.50 (m, 1H). ^{13}C NMR (δ/ppm , 125 MHz, DMSO- d_6): 29.6, 35.6, 37.0, 38.7, 46.2, 57.7, 71.6, 115.8, 121.4, 127.2, 128.3, 128.4, 128.5, 130.0, 130.1, 131.3, 131.8, 131.9, 133.7, 134.3, 138.2, 143.4, 161.4. Anal. $\text{C}_{25}\text{H}_{25}\text{BrCl}_2\text{FNO}_3$: C, H, N.

rac-(1S,2R,4S)-N-[1-(3-Bromobenzyl)-2-hydroxy-4-(3-methylbutylsulfanyl)pentyl]-3-methylsulfanylpropionamide (16a). A solution of 3-methylsulfanylpropionic acid (42 mg, 0.35 mmol) and **15a** (125 mg, 0.33 mmol) in 40 mL of anhydrous THF was cooled to 0°C . Hydroxybenzotriazole (53 mg, 0.39 mmol) and EDC (70 mg, 0.35 mmol) were then added sequentially. The reaction mixture was stirred for 2 h at 0°C , warmed to 25°C , and stirred for a further 2 h. The organic phase was quenched with saturated NaHCO_3 and washed with brine. After extraction with Et_2O (3×50 mL), the combined organic layers were dried with MgSO_4 , filtered, and evaporated in vacuo. The resulting material was submitted to flash silica

gel chromatography, eluting with cyclohexane/EtOAc 2:1 to afford 133 mg (81%) of **16a** as a white solid. ^1H NMR (δ/ppm , 500 MHz, DMSO- d_6): 0.86 (d, $J = 0.9$ Hz, 3H), 0.88 (d, $J = 1.0$ Hz, 3H), 1.27 (d, $J = 6.9$ Hz, 3H), 1.41 (m, 3H), 1.63 (m, 2H), 1.99 (s, 3H), 2.25 (m, 2H), 2.49 (m, 5H), 2.92 (m, 1H), 2.99 (dd, $J = 13.8, 3.3$ Hz, 1H), 3.59 (m, 1H), 3.78 (m, 1H), 4.77 (d, $J = 6.7$ Hz, 1H), 7.20 (m, 2H), 7.34 (m, 1H), 7.41 (s, 1H), 7.71 (d, $J = 9.0$ Hz, 1H). ^{13}C NMR (δ/ppm , 125 MHz, DMSO- d_6): 14.5, 22.0, 23.0, 26.9, 27.0, 39.4, 35.3, 35.6, 36.9, 38.6, 40.1, 55.1, 70.6, 121.1, 128.1, 128.5, 128.8, 131.8, 142.4, 170.5. HRMS (ESI) m/z : $\text{C}_{21}\text{H}_{35}\text{BrNO}_2\text{S}_2$ (MH^+) calcd, 476.1254; found, 476.1292. Anal. $\text{C}_{21}\text{H}_{34}\text{BrNO}_2\text{S}_2$: C, H, N.

rac-(1S,2R,4S)-N-[1-(3-Bromobenzyl)-4-(4-fluorophenylsulfanyl)-2-hydroxy-6-methylheptyl]-2-(2,6-dimethylphenoxy)acetamide (16b). Coupling of **15b** (145 mg, 0.33 mmol) with (2,6-dimethylphenoxy)acetic acid (63 mg, 0.35 mmol) was used to prepare **16b** with 75% yield, as described for **16a**. ^1H NMR (δ/ppm , 500 MHz, DMSO- d_6): 0.82 (d, $J = 6.5$ Hz, 3H), 0.84 (d, $J = 6.4$ Hz, 3H), 1.35 (m, 2H), 1.57 (m, 2H), 1.84 (m, 1H), 2.16 (s, 6H), 2.79 (dd, $J = 13.7, 10.7$ Hz, 1H), 3.07 (dd, $J = 13.9, 3.0$ Hz, 1H), 3.30 (m, 1H), 3.96 (m, 1H), 3.96 (m, 1H), 3.96 (d, $J = 14.3$ Hz, 1H), 4.11 (d, $J = 14.3$ Hz, 1H), 5.10 (d, $J = 6.4$ Hz, 1H), 6.93 (dd, $J = 7.2, 6.7$ Hz, 1H), 7.02 (d, $J = 7.3$ Hz, 2H), 7.20 (m, 4H), 7.44 (m, 4H), 7.95 (m, 1H). ^{13}C NMR (δ/ppm , 125 MHz, DMSO- d_6): 15.7, 22.1, 22.3, 24.7, 35.0, 38.7, 44.1, 45.3, 55.9, 59.6, 70.1, 116.5, 121.1, 124.2, 128.1, 128.6, 128.7, 128.7, 129.3, 129.9, 130.1, 131.8, 133.5, 135.1, 142.3, 154.3, 161.4, 167.3. Anal. $\text{C}_{31}\text{H}_{37}\text{BrFNO}_3\text{S}$: C, H, N.

Synthesis of Compounds 16c–e. **rac-(1S,2R,4S)-N-[1-(3-Bromobenzyl)-6-(2,4-dichlorophenyl)-4-(4-fluorophenylsulfanyl)-2-hydroxyhexyl]-2-(2,4-dichlorophenoxy)acetamide (16c)**, **rac-(1S,2R,4S)-N-[1-(3-bromobenzyl)-6-(2,4-dichlorophenyl)-4-(4-fluorophenylsulfanyl)-2-hydroxyhexyl]-4,5-dimethoxybenzamide (16d)**, and a diastereomeric mixture of ((2R),1S,2R,4S)- and ((2R),1R,2S,4R)-tetrahydrofuran-2-carboxylic acid [1-(3-bromobenzyl)-6-(2,4-dichlorophenyl)-4-(4-fluorophenylsulfanyl)-2-hydroxyhexyl]amide (**16e**) were prepared in analogous fashion as **16a**, coupling **15c** with three distinct carboxylic acids as R_3 -fragments (0.35 mmol) with 84% (**16c**), 81% (**16d**), and 77% (**16e**) yield.

16c. ^1H NMR (δ/ppm , 500 MHz, DMSO- d_6): 1.63 (m, 2H), 1.76 (m, 2H), 2.66 (dd, $J = 14.0, 10.6$ Hz, 1H), 2.83 (m, 2H), 3.06 (dd, $J = 14.0, 3.4$ Hz, 1H), 3.29 (m, 1H), 3.87 (m, 1H), 3.96 (m, 1H), 4.47 (s, 2H), 5.01 (d, $J = 7.0$ Hz, 1H), 6.75 (d, $J = 8.9$ Hz, 1H), 7.16 (m, 2H), 7.20 (m, 2H), 7.33 (m, 2H), 7.38 (m, 2H), 7.47 (m, 1H), 7.42 (s, 1H), 7.47 (m, 2H), 7.50 (s, 1H), 7.53 (d, $J = 9.1$ Hz, 1H). ^{13}C NMR (δ/ppm , 125 MHz, DMSO- d_6): 29.5, 35.2, 35.3, 38.1, 45.8, 54.9, 67.7, 69.8, 115.1, 115.8, 121.2, 122.5, 125.0, 127.2, 127.6, 128.0, 128.5, 128.6, 129.0, 129.3, 129.9, 130.2, 130.7, 130.7, 134.8, 138.0, 142.0, 152.3, 161.5, 166.2. HRMS (ESI) m/z : $\text{C}_{33}\text{H}_{30}\text{BrCl}_4\text{FNO}_3\text{S}$ (MH^+) calcd, 757.9833; found, 757.9867.

16d. ^1H NMR (δ/ppm , 500 MHz, DMSO- d_6): 1.79 (m, 3H), 1.89 (m, 1H), 2.66 (dd, $J = 14.2, 11.1$ Hz, 1H), 2.83 (m, 2H), 3.20 (m, 1H), 3.39 (m, 1H), 3.74 (s, 3H), 3.78 (s, 3H), 3.88 (m, 1H), 4.15 (m, 1H), 5.00 (d, $J = 6.9$ Hz, 1H), 6.52 (s, 1H), 7.10 (m, 3H), 7.30 (m, 4H), 7.38 (m, 1H), 7.48 (m, 4H), 8.06 (d, $J = 6.9$ Hz, 1H). ^{13}C NMR (δ/ppm , 125 MHz, DMSO- d_6): 29.4, 35.5, 35.7, 38.5, 46.0, 55.6, 55.7, 56.1, 70.7, 109.4, 112.0, 115.7, 116.5, 121.2, 128.2, 128.5, 128.6, 129.7, 130.0, 130.9, 131.1, 131.8, 131.9, 133.7, 134.4, 134.5, 138.1, 142.6, 147.7, 149.9, 161.4, 166.3. HRMS (ESI) m/z : $\text{C}_{34}\text{H}_{33}\text{Br}_2\text{Cl}_2\text{FNO}_4\text{S}$ (MH^+) calcd, 797.9813; found, 797.9858. Anal. $\text{C}_{34}\text{H}_{32}\text{Br}_2\text{Cl}_2\text{FNO}_4\text{S}$: C, H, N.

16e (ratio of diastereomers 1:1). ^1H NMR (δ/ppm , 500 MHz, DMSO- d_6): 1.41 (m, 1H), 1.68 (m, 6H), 1.98 (m, 1H), 2.72 (m, 1H), 2.84 (m, 2H), 3.07 (m, 1H), 3.29 (m, 1H), 3.47 (m, 1H), 3.85 (m, 3H), 4.03 (m, 1H), 5.00 (d, $J = 6.5$ Hz, 1H), 7.17 (m, 2H), 7.34 (m, 3H), 7.39 (m, 4H), 7.48 (m, 3H). ^{13}C NMR (δ/ppm , 125 MHz, DMSO- d_6): 25.0, 29.1, 29.2, 34.6, 38.8, 45.3, 53.9, 67.3, 68.7, 76.9, 115.3, 120.5, 126.6, 127.3, 127.8, 127.9, 129.2, 130.7, 131.3, 133.0, 133.2, 134.0, 134.6, 137.4, 141.8, 161.0, 171.3. Anal. $\text{C}_{30}\text{H}_{32}\text{BrCl}_2\text{FNO}_3\text{S}$: C, H, N.

rac-(1S,2R,4S)-N-[1-(3-Bromobenzyl)-2-hydroxy-4-(3-methylbutane-1-sulfonyl)pentyl]-3-methanesulfonylpropanamide (17a). To a solution of **16a** (100 mg, 0.21 mmol) in 50 mL of CHCl₃ was added mCPBA (200 mg, 1.26 mmol, 6 equiv) sequentially. The reaction mixture was heated for 2 h under reflux. The reaction was quenched by pouring into saturated NaHCO₃, and the product was extracted with CH₂-Cl₂. The organic layer was washed with NaHCO₃ (6 × 50 mL) and then with brine. After drying (MgSO₄), the solvent was evaporated and the residue purified by flash chromatography on silica gel using 3:1 cyclohexane/EtOAc to give 95 mg (89%) of **17a**. ¹H NMR (δ/ppm, 500 MHz, DMSO-*d*₆): 0.91 (d, *J* = 6.5 Hz, 6H), 1.34 (d, *J* = 6.8 Hz, 3H), 1.43 (ddd, *J* = 15.2, 8.2, 7.0 Hz, 1H), 1.57 (m, 2H), 1.68 (m, 2H), 2.17 (ddd, *J* = 14.8, 4.5, 4.0 Hz, 1H), 2.46 (m, 2H), 2.55 (dd, *J* = 13.0, 10.3 Hz, 1H), 2.87 (s, 3H), 2.96 (dd, *J* = 13.9, 3.4 Hz, 1H), 3.15 (m, 2H), 3.27 (m, 1H), 3.62 (m, 1H), 3.86 (m, 1H), 5.04 (m, 1H), 7.22 (m, 2H), 7.36 (m, 1H), 7.43 (s, 1H), 8.01 (d, *J* = 9.0 Hz, 1H). ¹³C NMR (δ/ppm, 125 MHz, DMSO-*d*₆): 14.7, 21.9, 26.7, 27.9, 29.2, 33.2, 34.6, 46.9, 49.8, 54.9, 55.1, 62.7, 71.0, 121.2, 128.2, 128.6, 130.0, 131.8, 142.1, 168.4. HRMS (ESI) *m/z*: C₂₁H₃₄BrNO₆S₂ calcd, 540.1058; found, 540.1089. Anal. C₂₁H₃₄BrNO₆S₂: C, H, N.

Synthesis of Compounds 17 b–e. *rac*-(1S,2R,4S)-N-[1-(3-Bromobenzyl)-4-(4-fluorobenzenesulfonyl)-2-hydroxy-6-methylheptyl]-2-(2,6-dimethylphenoxy)acetamide (**17b**), *rac*-(1S,2R,4S)-N-[1-(3-bromobenzyl)-6-(2,4-dichlorophenyl)-4-(4-fluorobenzenesulfonyl)-2-hydroxyhexyl]-2-(2,4-dichlorophenoxy)acetamide (**17c**), *rac*-(1S,2R,4S)-2-bromo-*N*-[1-(3-bromobenzyl)-6-(2,4-dichlorophenyl)-4-(4-fluorobenzenesulfonyl)-2-hydroxyhexyl]-4,5-dimethoxybenzamide (**17d**), and the separated diastereomers ((2*R*),1*S*,2*R*,4*S*)- and ((2*R*),1*R*,2*S*,4*R*)-tetrahydrofuran-2-carboxylic acid [1-(3-bromobenzyl)-6-(2,4-dichlorophenyl)-4-(4-fluorophenylsulfanyl)-2-hydroxyhexyl]amide (**17e**) were prepared analogously as **17a**, however, with only 3 equiv of mCPBA (0.63 mmol) oxidizing **16b–e** to give 80% (**17b**), 89% (**17c**), 90% (**17d**), and 87% (**17e**) yields, respectively.

17b. ¹H NMR (δ/ppm, 500 MHz, DMSO-*d*₆): 0.75 (d, *J* = 6.4 Hz, 3H), 0.85 (d, *J* = 6.7 Hz, 3H), 1.26 (m, 2H), 1.44 (m, 1H), 1.66 (m, 1H), 2.08 (m, 1H), 2.16 (s, 6H), 2.75 (dd, *J* = 11.0, 2.5 Hz, 1H), 3.03 (dd, *J* = 13.9, 3.4 Hz, 1H), 3.41 (m, 1H), 3.76 (m, 1H), 3.96 (m, 1H), 3.96 (d, *J* = 14.5 Hz, 1H), 4.10 (d, *J* = 14.5 Hz, 1H), 5.25 (d, *J* = 6.9 Hz, 1H), 6.94 (d, *J* = 7.1 Hz, 1H), 7.01 (d, *J* = 7.1 Hz, 2H), 7.21 (m, 2H), 7.36 (dd, *J* = 7.4, 1.4 Hz, 1H), 7.44 (s, 1H), 7.51 (d, *J* = 9.0 Hz, 2H), 7.93 (m, 3H). ¹³C NMR (δ/ppm, 125 MHz, DMSO-*d*₆): 15.6, 20.9, 23.1, 24.3, 33.3, 34.9, 38.8, 54.9, 59.0, 70.0, 70.6, 116.5, 121.1, 124.2, 128.1, 128.6, 128.7, 129.9, 130.2, 131.6, 131.8, 133.7, 142.3, 154.2, 165.0, 167.3. Anal. C₃₁H₃₇BrFNO₅S: C, H, N.

17c. ¹H NMR (δ/ppm, 500 MHz, DMSO-*d*₆): 1.65 (m, 2H), 1.99 (m, 1H), 2.10 (ddd, *J* = 15.2, 2.7 Hz, 1H), 2.61 (dd, *J* = 13.6, 10.7 Hz, 1H), 2.70 (m, 2H), 3.01 (dd, *J* = 13.9, 3.0 Hz, 1H), 3.42 (m, 1H), 3.69 (m, 1H), 3.96 (m, 1H), 4.48 (s, 2H), 5.18 (d, *J* = 6.7 Hz, 1H), 6.74 (d, *J* = 8.9 Hz, 1H), 7.20 (m, 3H), 7.33 (m, 2H), 7.38 (m, 2H), 7.47 (m, 3H), 7.54 (d, *J* = 2.6 Hz, 1H), 7.81 (d, *J* = 9.3 Hz, 1H), 7.92 (m, 2H). ¹³C NMR (δ/ppm, 125 MHz, DMSO-*d*₆): 28.8, 29.0, 32.2, 34.6, 54.5, 60.0, 67.4, 70.5, 114.9, 116.2, 121.0, 122.3, 124.8, 127.0, 127.5, 127.8, 128.3, 128.4, 128.9, 129.0, 129.7, 131.2, 131.3, 131.5, 131.6, 133.4, 136.9, 141.5, 152.9, 164.7, 166.0. HRMS (ESI) *m/z*: C₃₃H₃₀BrCl₄FNO₅S (MH⁺) calcd, 789.9755; found, 789.9766. Anal. C₃₃H₂₉BrCl₄FNO₅S: C, H, N.

17d. ¹H NMR (δ/ppm, 500 MHz, DMSO-*d*₆): 1.65 (m, 1H), 1.73 (ddd, *J* = 14.9, 10.7, 4.0 Hz, 1H), 1.94 (m, 1H), 2.42 (ddd, *J* = 15.3, 7.8, 2.5 Hz, 1H), 2.65 (m, 2H), 3.18 (dd, *J* = 14.0, 3.2 Hz, 1H), 3.46 (m, 1H), 3.75 (m, 1H), 3.75 (s, 3H), 3.78 (s, 3H), 4.03 (m, 1H), 5.23 (d, *J* = 7.1 Hz, 1H), 6.59 (s, 1H), 7.10 (s, 1H), 7.27 (m, 2H), 7.33 (m, 3H), 7.38 (m, 3H), 7.49 (m, 1H), 7.89 (m, 2H), 8.17 (d, *J* = 9.4 Hz, 1H). ¹³C NMR (δ/ppm, 125 MHz, DMSO-*d*₆): 29.0, 29.5, 32.6, 35.4, 55.5, 55.7, 56.0, 60.0, 71.5, 109.3, 111.7, 115.7, 116.5, 121.2, 127.3, 128.2, 128.6, 128.6, 130.0, 130.7, 131.4, 131.5, 131.6, 131.9, 133.6, 137.2, 142.3, 147.6, 149.8, 166.0, 166.5. HRMS (ESI) *m/z*: C₃₄H₃₃-

Br₂Cl₂FNO₆S (MH⁺) calcd, 829.9736; found, 829.9756. Anal. C₃₄H₃₂Br₂Cl₂FNO₆S: C, H, N.

The diastereomeric mixture of **17e** was separated into the ((2*R*),1*S*,2*R*,4*S*)- and ((2*R*),1*R*,2*S*,4*R*)-diastereomers via chiral HPLC. Assignment of the absolute configuration to the different diastereomers was performed with respect to their IC₅₀ values in the HIV protease assay (4.2 μM for the ((2*R*),1*S*,2*R*,4*S*)-diastereomer and > 40 μM for the ((2*R*),1*R*,2*S*,4*R*)-diastereomer) and similarity to the crystallographically fully characterized **17b** and the small molecule crystal structure of *rac*-**19**.

((2R),1S,2R,4S)-17e. ¹H NMR (δ/ppm, 300 MHz, CDCl₃): 1.87 (m, 6H), 2.28 (m, 2H), 2.56 (ddd, *J* = 13.8, 9.3, 7.2 Hz, 1H), 2.90 (m, 3H), 3.32 (m, 1H), 3.82 (m, 2H), 3.89 (m, 1H), 4.06 (m, 1H), 4.27 (dd, *J* = 8.1, 5.8 Hz, 1H), 5.56 (m, 1H), 6.86 (d, *J* = 7.2 Hz, 1H), 7.17 (m, 7H), 7.34 (s, 1H), 7.39 (m, 1H), 7.83 (m, 2H). ¹³C NMR (δ/ppm, 125 MHz, CDCl₃): 25.2, 29.6, 29.8, 30.2, 31.9, 35.3, 57.3, 60.4, 69.5, 71.9, 78.2, 116.8, 122.7, 127.2, 127.8, 129.4, 130.0, 130.3, 131.4, 131.5, 131.6, 132.3, 132.9, 133.5, 134.3, 136.3, 140.0, 164.9, 174.9. Anal. C₃₀H₃₂BrCl₂FNO₅S: C, H, N.

((2R),1R,2S,4R)-17e. ¹H NMR (δ/ppm, 300 MHz, CDCl₃): 1.50 (m, 1H), 1.75 (m, 4H), 2.02 (m, 1H), 2.17 (m, 2H), 2.57 (ddd, *J* = 13.7, 9.3, 7.3 Hz, 1H), 2.71 (dd, *J* = 14.0, 10.7 Hz, 1H), 2.84 (ddd, *J* = 13.8, 9.3, 4.7 Hz, 1H), 3.03 (dd, *J* = 14.2, 4.5 Hz, 1H), 3.36 (m, 1H), 3.66 (m, 1H), 3.79 (m, 1H), 4.03 (m, 1H), 4.14 (m, 1H), 4.28 (dd, *J* = 8.3, 5.3 Hz, 1H), 6.72 (d, *J* = 7.7 Hz, 1H), 7.17 (m, 7H), 7.37 (s, 1H), 7.40 (m, 1H), 7.83 (m, 2H). ¹³C NMR (δ/ppm, 125 MHz, CDCl₃): 25.5, 29.9, 30.2, 30.5, 32.2, 36.2, 56.3, 60.8, 69.9, 72.2, 78.5, 116.8, 123.0, 127.6, 128.2, 129.8, 130.3, 130.7, 131.9, 132.0, 132.6, 133.3, 133.7, 134.8, 136.7, 140.3, 164.9, 175.0. HRMS (ESI) *m/z*: C₃₀H₃₂BrCl₂FNO₅S (MH⁺) calcd, 686.0549; found, 686.0545. Anal. C₃₀H₃₂BrCl₂FNO₅S: C, H, N.

rac-(1S,2R,4S)-N-[1-Bromobenzyl]-2-hydroxy-6-methyl-4-(4-methylaminobenzenesulfonyl)heptyl]-2-(2,6-dimethylphenoxy)acetamide (18a). To a solution of **17b** (50 mg, 0.08 mmol) was added 10 mL (1 M in THF) of MeNH₂. The reaction mixture was transferred to an autoclave and heated to 160 °C and 2 bar. After being stirred for 5 h, the reaction was quenched with 50 mL of water and extracted with Et₂O (3 × 40 mL). The combined organic layers were dried (MgSO₄), filtrated, and evaporated under reduced pressure. The crude product was flash chromatographed with cyclohexane/EtOAc (3:1) to give 45 mg (87%) of **18a** as a light brown solid. ¹H NMR (δ/ppm, 500 MHz, DMSO-*d*₆): 0.78 (d, *J* = 6.3 Hz, 3H), 0.85 (d, *J* = 6.6 Hz, 3H), 1.16 (m, 1H), 1.36 (m, 1H), 1.48 (m, 1H), 1.65 (m, 1H), 2.04 (ddd, *J* = 15.3, 2.8, 7.2 Hz, 1H), 2.17 (s, 6H), 2.71 (d, *J* = 4.7 Hz, 3H), 2.76 (dd, *J* = 13.6, 2.5 Hz, 1H), 3.03 (dd, *J* = 14.0, 2.7 Hz, 1H), 3.22 (m, 1H), 3.77 (m, 1H), 3.96 (m, 1H), 3.96 (d, *J* = 14.6 Hz, 1H), 4.12 (d, *J* = 14.6 Hz, 1H), 5.14 (d, *J* = 6.6 Hz, 1H), 6.62 (d, *J* = 8.9 Hz, 2H), 6.66 (d, *J* = 4.7 Hz, 1H), 6.94 (dd, *J* = 8.2, 7.0 Hz, 1H), 7.01 (dd, *J* = 7.3, 6.6 Hz, 2H), 7.22 (m, 2H), 7.35 (dd, *J* = 7.6, 1.3 Hz, 1H), 7.48 (s, 1H), 7.49 (d, *J* = 9.0 Hz, 2H), 7.75 (d, *J* = 9.7 Hz, 1H). ¹³C NMR (δ/ppm, 125 MHz, DMSO-*d*₆): 15.6, 21.1, 23.2, 24.3, 28.9, 33.7, 34.9, 35.1, 54.9, 59.2, 70.0, 70.9, 110.5, 121.3, 124.2, 128.2, 128.6, 128.7, 129.9, 130.2, 130.3, 130.4, 131.8, 142.3, 153.6, 154.3, 167.2. Anal. C₃₂H₄₁BrN₂O₅S: C, H, N.

rac-(1S,2R,4S)-N-[1-Bromobenzyl]-4-(4-(dimethylamino)benzenesulfonyl)-2-hydroxy-6-methylheptyl]-2-(2,6-dimethylphenoxy)acetamide (18b) was prepared in the same manner from **17b**, however, using Me₂NH (10 mL, 1 M in THF) for nucleophilic substitution to give 47 mg of **18b** (90%) as a light brown solid: ¹H NMR (δ/ppm, 500 MHz, DMSO-*d*₆): 0.78 (d, *J* = 6.3 Hz, 3H), 0.85 (d, *J* = 6.5 Hz, 3H), 1.16 (m, 1H), 1.36 (m, 1H), 1.48 (m, 1H), 1.66 (m, 1H), 2.04 (m, 1H), 2.16 (s, 6H), 2.75 (dd, *J* = 16.2, 2.9 Hz, 1H), 2.99 (s, 6H), 3.03 (dd, *J* = 13.6, 3.2 Hz, 1H), 3.23 (m, 1H), 3.76 (m, 1H), 3.96 (m, 1H), 3.96 (d, *J* = 14.3 Hz, 1H), 4.11 (d, *J* = 14.2 Hz, 1H), 5.14 (s, 1H), 6.78 (d, *J* = 9.2 Hz, 2H), 6.94 (dd, *J* = 8.0, 7.0 Hz, 1H), 7.01 (dd, *J* = 7.3, 7.3 Hz, 2H), 7.22 (m, 2H), 7.36 (dd, *J* = 7.6, 1.9 Hz, 1H), 7.44 (s, 1H), 7.56 (d, *J* = 9.0

Hz, 2H), 7.85 (d, $J = 9.7$ Hz, 1H). ^{13}C NMR (δ/ppm , 125 MHz, DMSO- d_6): 15.6, 21.1, 23.2, 24.3, 33.7, 34.9, 39.4, 54.9, 59.2, 70.1, 70.7, 110.7, 121.3, 124.1, 128.2, 128.6, 128.7, 129.9, 130.1, 130.2, 130.3, 131.8, 142.3, 153.0, 154.3, 167.2. Anal. $\text{C}_{33}\text{H}_{43}\text{BrN}_2\text{O}_5\text{S}$: C, H, N.

rac-(4S,5R,2S)-4-(3-Bromobenzyl)-5-[-(2,4-dichlorophenyl)-2-(4-fluorobenzenesulfonyl)butyl]-1,3-oxazolidin-2-one (19) was prepared by oxidation of **14 c** (100 mg, 0.17 mmol) with mCPBA (80 mg, 0.51 mmol, 3 equiv) in the same manner as **17b** to give 77 mg (74%) of **19**. ^1H NMR (δ/ppm , 500 MHz, DMSO): 1.72 (m, 1H), 1.96 (m, 1H), 2.12 (m, 2H), 2.70 (m, 2H), 2.87 (m, 2H), 3.44 (m, 1H), 4.19 (m, 1H), 4.76 (m, 1H), 7.31 (m, 2H), 7.37 (m, 2H), 7.49 (m, 5H), 7.74 (s, 1H), 7.89 (m, 2H). ^{13}C NMR (δ/ppm , 125 MHz, DMSO): 27.7, 28.7, 28.9, 34.7, 54.9, 60.0, 76.7, 116.7, 121.7, 127.4, 128.1, 128.6, 129.2, 130.5, 131.6, 131.7, 131.7, 132.0, 133.0, 133.6, 137.1, 140.3, 157.4, 165.2. Anal. $\text{C}_{26}\text{H}_{23}\text{BrCl}_2\text{NO}_4\text{S}$: C, H, N.

Acknowledgment. The authors are grateful to Bayer AG, Wuppertal, Germany, for financial support. We thank also Prof. Dieter Hoppe, Department of Organic Chemistry, University of Münster, Münster, Germany, for his supervision and helpful discussions during the first stages of the project. Additionally our thanks go to Prof. Andreas Pfaltz and Dr. Frederik Menges, Department of Organic Chemistry, University of Basel, Basel, Switzerland, for the permission to use their chiral HPLC. The clone of the protease was kindly provided by Prof. Helena Danielson, Department of Biochemistry, University of Uppsala, Uppsala, Sweden. We would also like to thank the beamline staff at Bessy II.

Supporting Information Available: Results from elemental analysis and crystallographic data for **19**. This material is available free of charge via the Internet at <http://pubs.acs.org>.

References

- Lien, E. J.; Gao, H.; Lien, L. L. In search of ideal antihypertensive drugs: Progress in five decades. *Prog. Drug Res.* **1994**, *43*, 43–86.
- Seiffers, M. J.; Miller, L. L.; Segal, H. L. Partial Characterization of Human Pepsin I, Pepsin IIA, Pepsin IIB, and Pepsin III. *Biochemistry* **1964**, *3*, 1203–1209.
- Gulnik, S.; Baldwin, E. T.; Tarasova, N.; Erickson, J. Human Liver Cathepsin D Purification, Crystallization and Preliminary X-ray Diffraction Analysis of a Lysosomal Enzyme. *J. Mol. Biol.* **1992**, *227*, 265–270.
- Silva, A. M.; Lee, A. Y.; Gulnik, S. V.; Maier, P.; Collins, J.; Bhat, T. N.; Collins, P. J.; Cachau, R. E.; Luker, K. E.; Gluzman, I. Y.; Francis, S. E.; Oksman, A.; Goldberg, D. E.; Erickson, J. W. Structure and inhibition of plasmepsin II, a haemoglobin-degrading enzyme from Plasmodium falciparum. *Proc. Natl. Acad. Sci. U.S.A.* **1996**, *93*, 10034–10039.
- Darke, P. L.; Huff, J. R. HIV protease as an inhibitor target for the treatment of AIDS. *Adv. Pharmacol. (San Diego)* **1994**, *5*, 399–454.
- Vassar, R.; Bennet, B. D.; Babu-Khan, S.; Kahn, S.; Mendiaz, E. A.; Denis, P.; Teplow, D. B.; Ross, S.; Amarante, P.; Loeloff, R.; Luo, Y.; Fisher, S.; Fuller, J.; Edneson, S.; Lile, J.; Jarosinski, M. A.; Biere, A. L.; Curran, E.; Burgess, T.; Louis, J.-C.; Collins, F.; Treanor, J.; Rogere, G.; Citron, M. Beta-secretase cleavage of Alzheimer's amyloid precursor protein by the transmembrane aspartic protease BACE. *Science* **1999**, *286*, 735–741.
- Rich, D. H.; Sun, E. T. O.; Ulm, E. Synthesis of analogues of the carboxyl protease inhibitor pepstatin; Effect of structure on inhibition of pepsin and renin. *J. Med. Chem.* **1980**, *23*, 27–33.
- Kim, E. E.; Baker, C. T.; Dwyer, M. D.; Murcko, M. A.; Rao, B. G.; Tung, R. D.; Navia, M. A. Crystal structure of HIV-1 protease in complex with VX-478, a potent and orally bioavailable inhibitor of the enzyme. *J. Am. Chem. Soc.* **1995**, *117*, 1181–1182.
- Bolis, G.; Fung, A. K. L.; Greer, J.; Kleinert, H. D.; Marcotte, P. A.; Perun, T. J.; Plattner, J. J.; Stein, H. H. Renin Inhibitors. Dipeptide analogues of angiotensinogen incorporating transition-state, nonpeptidic replacements at the scissile bond. *J. Med. Chem.* **1987**, *30*, 1729–1737.
- Lee, E. C.; Kick, E. K.; Ellman, J. A. General Solid-Phase Synthesis Approach To Prepare Mechanism-Based Aspartyl Protease Inhibitor Libraries. Identification of Potent Cathepsin D Inhibitors. *J. Am. Chem. Soc.* **1998**, *120*, 9735–9747.
- Ghosh, A. K.; Bilcer, G.; Harwood, C.; Kawahama, R.; Shin, D.; Hussain, K. A.; Hong, L.; Loy, J. A.; Nguyen, C.; Koelsch, G.; Ermoloff, J.; Tang, J. Structure-Based Design: Potent Inhibitors of Human Brain Memapsin 2 (β -Secretase). *J. Med. Chem.* **2001**, *44*, 2865–2868.
- Rodriguez, M.; Llinares, M.; Doulut, S.; Heitz, A.; Martinez, J. A facile synthesis of chiral *N*-protected β -amino alcohols. *Tetrahedron Lett.* **1991**, *32*, 923–926.
- Marx, M.; Tidwell, T. T. Reactivity-selectivity in the Swern oxidation of alcohols using dimethyl sulfoxide–oxalyl chloride. *J. Org. Chem.* **1984**, *49*, 788–793.
- Anh, N. T. Regio- and Stereoselectivities in some Nucleophile Reactions. *Top. Curr. Chem.* **1980**, *88*, 145–162.
- Cherest, M.; Felkin, H.; Prudent, N. Torsional Strain involving Partial Bonds: The Stereochemistry of the Lithium Aluminium Hydride Reductions of some simple Open-Chain Ketones. *Tetrahedron Lett.* **1968**, *18*, 2199–2204. (b) Cherest, M.; Felkin, H. Torsional Strain involving Partial Bonds: The Steric Course of the Reactions between Allyl Magnesium Bromide and 4-*tert*-Butyl-cyclohexanones. *Tetrahedron Lett.* **1968**, *18*, 2205–2208.
- Narasaka, K.; Pai, F.-C. Stereoselective reduction of β -hydroxyketones to 1,3-diols. *Tetrahedron* **1984**, *40*, 2233–2238.
- Vazquez, M. L.; Bryant, M. L.; Clare, M.; DeCrescenzo, G. A.; Doherty, E. M.; Freskos, J. N.; Geman, P. D.; Houseman, K. A.; Julien, J. A.; Kocan, G. P.; Mueller, R. A.; Shieh, H.-S.; Stallings, W. C.; Stegeman, R. A.; Talley, J. J. Inhibitors of HIV-1 Protease Containing the Novel and Potent (R)-Hydroxyethyl)sulfonylamide Isostere. *J. Med. Chem.* **1995**, *38*, 581–584.
- Beaulieu, P. L.; Anderson, P. C.; Cameron, D. R.; Croteau, G.; Gorys, V.; Grand-Maitre, C.; Lamarre, D.; Liard, F.; Paris, W.; Plamondon, L.; Soucy, F.; Thibeault, D.; Wernic, D.; Yoakim, C. 2',6'-Dimethylphenoxyacetyl: A new achiral high affinity $\text{P}_3\text{-P}_2$ ligand for peptidomimetic-based HIV protease inhibitors. *J. Med. Chem.* **2000**, *43*, 1094–1108.
- Gohlke, H.; Hendlich, M.; Klebe, G. Knowledge-based Scoring Function to Predict Protein–Ligand Interactions. *J. Mol. Biol.* **2000**, *295*, 337–356.
- Goodsell, D. S.; Morris, G. M.; and Olson, A. J. Docking of Flexible Ligands: Applications of AutoDock. *J. Mol. Recognit.* **1996**, *9*, 1–5.
- Morris, G. M.; Goodsell, D. S.; Halliday, R. S.; Huey, R.; Hart, W. E.; Belew, R. K.; Olson, W. E. Automated docking using a Lamarckian genetic algorithm and an empirical binding free energy function. *J. Comput. Chem.* **1998**, *14*, 1639–1662.
- Sotriffer, C. A.; Gohlke, H.; Klebe, G. Docking into Knowledge-Based Potential Fields: A Comparative Evaluation of DrugScore. *J. Med. Chem.* **2002**, *45*, 1967–1970.
- Baldwin, E. T.; Bhat, T. N.; Gulnik, S.; Hosur, M. V.; Sowder, D.; Cachau, R. E.; Collins, J.; Silva, A. M.; Erickson, J. W. Crystal structures of native and inhibited forms of human cathepsin D: Implications for lysosomal targeting and drug design. *Proc. Natl. Acad. Sci. U.S.A.* **1993**, *90*, 6796–6799.
- Agarwal, N.; Rich, D. H. Inhibition of cathepsin D by substrate analogues containing statine and by analogues of pepstatin. *J. Med. Chem.* **1986**, *29*, 2519–2524.
- Kempf, D. J. Dipeptide Analogues: Versatile Synthesis of the Hydroxyethylene Isoster. *J. Org. Chem.* **1986**, *51*, 3921–3926.
- Reetz, M. T. New Approaches to the Amino Acids as Chiral Building Blocks in Organic Synthesis. *Angew. Chem. Int. Ed. Engl.* **1991**, *12*, 1531–1546.
- Taylor, A.; Brown D. P.; Kadam, S.; Maus M.; Kohlbrenner W. E.; Weigl D.; Turon M. C.; Katz L. High-level expression and purification of mature HIV-1 protease in *Escherichia coli* under control of the araBAD promoter. *Appl. Microbiol. Biotechnol.* **1992**, *37*, 205–210.
- Toth, M. V.; Marshall, G. R. A simple continuous fluorometric assay for HIV Protease. *Int. J. Pept. Protein Res.* **1990**, *36*, 544–550.
- Otwinowski, Z.; Minor, W. Processing of X-ray Diffraction Data Collected in Oscillation Mode. *Methods Enzymol.* **1997**, *276A*, 307–326.
- Navaza, J. On the role of atomicity in direct methods: A new criterion for ab initio phase determination. *Acta Crystallogr. A* **1992**, *48*, 695–700.
- Unge, T. HIV-1 Protease in Complex with the Inhibitor Bea403. (to be published)
- Sheldrick, G. M.; Schneider, T. R. SHELXL: High-Resolution Refinement. *Methods Enzymol.* **1997**, *277A*, 319–343.
- Jones, T. A.; Zou, J. Y.; Cowan, S. W.; Kjeldgaard, M. Improved methods for building protein models in electron density maps and the location of errors in these models. *Acta Crystallogr. A* **1991**, *47*, 110–119.